

Solving Parametric PDEs with Radial Basis Functions and Deep Neural Networks[†]

Guanhang Lei, Zhen Lei, Lei Shi, and Chenyu Zeng

School of Mathematical Sciences,
Shanghai Key Laboratory for Contemporary Applied Mathematics,
Fudan University, Shanghai, 200433, P. R. China
Email: ghlei21@m.fudan.edu.cn
{zlei, leishi, cyzeng19}@fudan.edu.cn

April 15, 2024

Abstract

We propose the POD-DNN, a novel algorithm leveraging deep neural networks (DNN) along with radial basis functions (RBF) in the context of the proper orthogonal decomposition (POD) reduced basis method (RBM), aimed at approximating the parametric mapping of parametric partial differential equations on irregular domains. The POD-DNN algorithm capitalizes on the low-dimensional characteristics of the solution manifold for parametric equations, alongside the inherent offline-online computational strategy of RBM and DNNs. In numerical experiments, POD-DNN demonstrates significantly accelerated computation speeds during the online phase. Compared to other algorithms that utilize RBF without integrating DNNs, POD-DNN substantially improves the computational speed in the online inference process. Furthermore, under reasonable assumptions, we have rigorously derived upper bounds on the complexity of approximating parametric mappings with POD-DNN, thereby providing a theoretical analysis of the algorithm's empirical performance.

Keywords: Parametric Partial Differential Equation; Reduced Basis Method; Proper Orthogonal Decomposition; Deep Neural Network; Radial Basis Function; Approximation Analysis.

1 Introduction

Parametric partial differential equations (PDEs) are widely employed in depicting or modeling intricate phenomenon within various fields of science and engineering. These equations use parameters to account for variations in physical properties, geometric configurations, and

[†] The work described in this paper is supported by the Shanghai Science and Technology Program [Project No. 21JC1400600] and National Natural Science Foundation of China (Grants Nos.12171039 and 12061160462). The work of Zhen Lei is also supported by the New Cornerstone Science Foundation through the XPLOERER PRIZE and Sino-German Center Mobility Programme (Project No. M-0548).

initial or boundary conditions. For instance, within the realm of fluid mechanics, parametric PDEs are pivotal in representing how both liquids and gases move, enabling the simulation of diverse scenarios, like turbulence, wave propagation, and the interaction between different fluid layers, with equation parameters used to describe fluid attributes like viscosity and density, as well as external forces and boundary conditions. Directly solving parametric PDEs is possible via established discretization techniques, including the finite element, spectral, and finite volume methods. However, these methods often require fine discretization (e.g., fine meshing of the solution region) and solving linear systems with thousands of degrees of freedom to obtain sufficiently accurate solutions, leading to uncontrollable demands on computational resources. Additionally, in many practical applications in science and engineering, we often need to solve parametric PDEs in real-time against multiple queries, necessitating repeated and expensive computations, thus further increasing computational costs. In such cases, there is a need to develop efficient numerical methods that allow for rapid simulation of solutions when the equation parameters change.

The reduced basis method (RBM) is widely applied to the numerical simulations of large-scale problems involving parametric PDEs [16]. Intuitively, the solutions to parametric PDEs are often determined by several equation parameters, indicating that the solutions associated with all possible parameters constitute a low-dimensional manifold within the solution space. RBM partitions the numerical solution process into offline/online stages. In the offline phase, which typically incurs a relatively higher computational cost, we fully exploit this low-dimensional nature and use some precomputed solutions, i.e., snapshots, to construct what is known as the reduced basis space, a low-dimensional approximation space. During the online phase, we leverage this set of basis functions to form a small-scale algebraic system that can be solved in real time, thus enabling efficient numerical solving of the equation when input parameters change. Based on the low-dimensional assumption of the solution manifold, the solution for any query parameter values can be approximated by the span of these snapshots in the low-dimensional space. Once the low-dimensional space is established, the solution for new parameter values is efficiently solved in the online phase.

Given new parameters, RBM calculates the coefficients of the associated solution under the span of this reduced basis in the online phase. This parameters-coefficients relation can be seen as the so-called parametric map. Although we only need to solve a relatively small-scale linear system in the online phase, the computational cost remains prohibitively expensive for some large-scale practical problems. To further decrease the response time and enhance the efficiency of numerical simulations, we can train deep neural networks (DNNs) to directly learn the parametric map, thereby transforming the online calculation into a feedforward computation within the networks. The DNN-based approach retains the offline-online decomposition feature, and integrating DNN with RBM significantly diminishes the computational expenses during the online phase, albeit at the cost of introducing an additional stage of neural network training in the offline phase. This additional step usually consumes less time compared to constructing the low-dimensional approximation space. Moreover, this end-to-end DNN methodology facilitates the parallel processing of multiple parameters, offering further benefits when simultaneously handling various parameters.

Deep learning techniques have been successfully applied to develop efficient methods for solving PDEs. For example, DNN has been effectively implemented across various numerical PDE challenges. The deep Ritz method (DRM) [5] and physics-informed neural networks (PINNs) [17, 19] have been designed to train neural networks with functional-type losses to ap-

proximate underlying PDEs’ solutions directly. Neural operator methods like DeepONet [14] and Fourier neural operator (FNO) [13] employ a supervised learning framework in infinite-dimensional input and output function spaces. They utilize various encoding and decoding techniques to simplify the operator regression task into learning within finite-dimensional tensor spaces. Neural operators are trained to learn the PDE solution operators, eliminating the need to train a new neural network for each new input function. Deep learning methods have also been extensively investigated and widely utilized in parametrized systems [7, 20, 3, 9, 6, 11, 12].

This paper explores combining RBM with DNNs to design efficient numerical algorithms for solving the parametric maps of parametric PDEs. Learning a parametric map is closely akin to the neural operator method; the latter could be viewed as a generalization of the former. In our algorithmic design, the RBM method employs the low intrinsic dimensionality of the solution manifold to establish efficient encoding and decoding processes. Coupled with the powerful representational and approximation capabilities of DNNs, we can develop robust solvers for parametric maps. Additionally, we note that, compared to simulating the solution map of a general PDE in an infinite-dimensional function space, solving a parametric map only involves a finite-dimensional parameter space. This characteristic can facilitate designing a more efficient deep learning scheme for the parametric PDE problem.

Constructing an efficient RBM is central to designing numerical solutions for parametric maps. The classical RBM was initially integrated with the Galerkin method to solve parametric PDEs that exhibit affine dependence on parameters. Subsequently, reduced collocation methods (RCMs) were developed based on the collocation approach. RCMs offer greater flexibility and efficiency, reducing the online computational cost of solving nonlinear parametric PDEs using the Galerkin approach. Traditional collocation methods, such as pseudospectral methods [8], often require highly structured grids, which may be inconvenient for solving PDEs with irregularly shaped domains. In this paper, to further address the challenges of solving parametric PDEs in irregular domains, motivated by previous work [1], we utilize radial basis functions (RBFs) to construct a meshless RCM. RBF methods have been extensively employed for scattered data interpolation and approximation in high dimensions [21]. Unlike traditional pseudospectral methods, RBF methods are collocation methods implemented on scattered sets of collocation sites and are not confined to any particular geometric structure. Typically, RBF methods approximate differential operators using global stencils, but our approach uses a local technique. Inspired by its similarity to finite difference (FD) methods, this is referred to as the RBF-FD method. Based on RBF-FD, we construct the low-dimensional reduced basis space. Popular approaches in this step include the greedy algorithm [15] and the proper orthogonal decomposition (POD) [2, 18, 10]. The greedy algorithm selects one optimal parameter and its associated snapshot by a posteriori error estimate at each iterative step. POD is based on the classic singular value decomposition (SVD) of a matrix, which directly extracts the main part of the snapshot matrix.

In this paper, we approximate the parametric maps of parametric PDEs on irregular domains through a synergistic combination of the RBF-FD method, POD-based RBM, and DNNs. Our algorithm capitalizes on the offline-online computational strategy inherent to DNNs, showcasing reduced computational costs in the online phase compared to RBF-based RCM proposed in [1], as evidenced by our numerical experiments. Furthermore, integrating RBM significantly reduces the output dimension of DNNs, facilitating easier network training, convergence, and inference processes. In addition to proposing an efficient deep

learning architecture for numerically solving the parametric maps of parametric PDEs, another contribution of this article is the rigorous derivation of the algorithm’s complexity upper bounds under reasonable assumptions, as seen in Theorem 1. Specifically, we establish the upper bounds for the depth and the number of non-zero parameters of the ReLU DNNs when approximating the mapping $\mu \mapsto \mathbf{c}(\mu)$ with precision $\varepsilon > 0$. Here, μ denotes the parameter of the parametric PDE, and $\mathbf{c}(\mu)$ represents the coefficient vector of the solution \mathbf{u}_μ within the span of the reduced basis. Our derived upper bounds indicate that the network’s depth is approximately $\mathcal{O}(\log_2(1/\varepsilon) \log_2(\log_2(1/\varepsilon)))$, and the number of non-zero parameters is $\mathcal{O}(n^3 \log_2^2(1/\varepsilon))$, where n is the dimension of the reduced basis. This bound on the number of non-zero parameters is better than the previous result $\mathcal{O}(n^3 \log_2^2(1/\varepsilon) \log_2^2(\log_2(1/\varepsilon)))$ in [11]. Our complexity analysis theoretically guarantees the efficiency of the novel deep learning algorithm we propose.

The rest of the paper is organized as follows. In Section 2, we briefly review the RBF-FD method and POD-based RBM for solving parametric PDEs in irregular domains. Section 3 introduces our novel algorithm, termed the POD-DNN algorithm (see Algorithm 1). This algorithm integrates the RBF-FD method, POD-based RBM, and DNNs to numerically simulate parametric maps. In Section 4, we commence with basic definitions and operations relevant to neural networks, leading to the proof of our main theorem, delineated as Theorem 1. The experimental validation of our algorithm is detailed in Section 5, where we also compare the numerical results with those obtained using the RBF-FD method and RBF-based RCM.

2 Preliminaries

2.1 Parametric PDEs in Irregular Domains

We consider the boundary value problem of parametric PDEs

$$\begin{cases} \mathcal{L}(\mu)u_\mu(x) = f(x; \mu), & x \in \Omega \subset \mathbb{R}^n, \\ \mathcal{B}(\mu)u_\mu(x) = g(x; \mu), & x \in \partial\Omega, \end{cases} \quad (2.1)$$

where $x \in \mathbb{R}^n$ represents the spatial variable, $\mu = (\mu_1, \dots, \mu_p) \in \mathcal{D} \subset \mathbb{R}^p$ with \mathcal{D} a prescribed p -dimensional real parameter domain, $\Omega \subset \mathbb{R}^n$ is an irregular domain with complex geometry, $\mathcal{L}(\mu)$ is a differential operator that depends on the parameter μ , $\mathcal{B}(\mu)$ is the boundary condition, and u_μ is the unknown solution associated with the parameter μ . For given functions f and g , we assume that (2.1) has a unique classical solution.

Traditional numerical solvers for PDEs are typically tailored to address single equations within regular domains. For instance, the finite difference (FD) method partitions a regular domain using uniform grids, transforming the unknown function into vector representation at grid points and recasting the equation as an algebraic relationship between matrices. However, this approach necessitates solving a distinct PDE for each parameter set, resulting in significant computational expense. In contrast, this paper adopts the radial basis function finite difference (RBF-FD) method to approximate the differential operator $\mathcal{L}(\mu)$ with a matrix $L(\mu)$. The RBF-FD method, being mesh-free, adeptly accommodates PDEs situated in irregular domains.

2.2 RBF-FD Method for PDE

In this subsection, we review the RBF-FD method for approximating linear differential operators in (2.1). Then, we discuss how the RBF-FD method can be used to discretize partial differential equations with Dirichlet boundary conditions. Readers may refer to [21] for definitions of RBF and conditionally positive definite function.

Let $\ell \in \mathbb{N}$ and

$$\Psi_{\ell-1} := \text{span} \left\{ p : \mathbb{R}^n \rightarrow \mathbb{R} \mid p(x) = \prod_{i=1}^n x_i^{\alpha_i}, \alpha_i \in \mathbb{N} \cup \{0\}, \sum_{i=1}^n \alpha_i \leq \ell - 1 \right\}$$

denotes the space of d -variate polynomials of degree at most $\ell - 1$. We consider a conditionally positive definite functions $\varphi : [0, \infty) \rightarrow \mathbb{R}$ of order ℓ and a $\Psi_{\ell-1}$ -unisolvant set of nodes $X = \{x_i\}_{i=1}^N \subset \Omega$, which contains interior and boundary nodes, i.e., $X = X_\Omega \cup X_{\partial\Omega}$ where $X_\Omega = \{x_1, \dots, x_{N_I}\} \subset \Omega$ and $X_{\partial\Omega} = \{x_{N_I+1}, \dots, x_N\} \subset \partial\Omega$. Let $X_i = \{x_{i_j} : j = 1, \dots, n_{\text{loc}}^i\} \subset X$ be the local set of neighboring points of x_i with $x_{i_1} = x_i$. X_i serves as a stencil for x_i . The point x_i is called the center node of the set X_i and $n_{\text{loc}}^i \in \mathbb{N}$ is the stencil size.

We then consider a linear partial differential operator \mathcal{L} and a sufficiently smooth function $u : \Omega \rightarrow \mathbb{R}$. The key idea of the RBF-FD method is to use a weighted sum of the function values at the nodes in the stencil X_i to represent the differential operator applied to the function u and evaluated locally at x_i , i.e.,

$$(\mathcal{L}u)(x_i) \approx \sum_{j=1}^{n_{\text{loc}}^i} w_j^i u(x_{i_j}). \quad (2.2)$$

Next, we demonstrate how these weights are computed for typical RBF spaces with (or without) polynomial augmentation. Let

$$\left\{ \varphi_{\epsilon, x_{i_j}} : \Omega \rightarrow \mathbb{R} \mid \varphi_{\epsilon, x_{i_j}} := \varphi(\epsilon \|x - x_{i_j}\|), \epsilon > 0, j = 1, \dots, n_{\text{loc}}^i \right\}$$

denote the n_{loc}^i RBFs associated with the shape parameter ϵ and the nodes of the stencil X_i . Define $Q := \dim \Psi_{\ell-1} = \binom{\ell + d - 1}{d}$ and we denote a basis of $\Psi_{\ell-1}$ by $\{p_1, \dots, p_Q\}$. RBFs associated with the stencil X_i and augmented by polynomials up to degree $\ell - 1$ have the following constrained function space:

$$\mathcal{R}_i := \left\{ s : \Omega \rightarrow \mathbb{R} \mid s(x) = \sum_{j=1}^{n_{\text{loc}}^i} \lambda_j^i \varphi_{\epsilon, x_{i_j}}(x) + \sum_{j=1}^Q \tilde{\lambda}_j^i p_j(x), \lambda_j^i, \tilde{\lambda}_j^i \in \mathbb{R} \right. \\ \left. \text{such that } \sum_{j=1}^{n_{\text{loc}}^i} \lambda_j^i p_k(x_{i_j}) = 0 \text{ for all } k \in \{1, \dots, Q\} \right\}.$$

For any function u , we can construct the interpolation function s_u from the space \mathcal{R}_i , by solving the following linear system

$$\tilde{A}^i \begin{bmatrix} \lambda^i \\ \tilde{\lambda}^i \end{bmatrix} := \begin{bmatrix} A^i & P^i \\ P^{iT} & \mathbf{0} \end{bmatrix} \begin{bmatrix} \lambda^i \\ \tilde{\lambda}^i \end{bmatrix} = \begin{bmatrix} u^i \\ \mathbf{0} \end{bmatrix} \quad (2.3)$$

where

$$\begin{aligned} A^i &:= [\varphi(\epsilon \|x_{i_j} - x_{i_k}\|)]_{jk} \in \mathbb{R}^{n_{\text{loc}}^i \times n_{\text{loc}}^i}, \quad P^i := [p_k(x_{i_j})]_{jk} \in \mathbb{R}^{n_{\text{loc}}^i \times Q}, \\ \lambda^i &:= [\lambda_1^i, \dots, \lambda_{n_{\text{loc}}^i}^i]^T, \quad \tilde{\lambda}^i := [\tilde{\lambda}_1^i, \dots, \tilde{\lambda}_Q^i]^T, \\ u^i &:= [u(x_{i_1}), \dots, u(x_{i_{n_{\text{loc}}^i}})]^T, \end{aligned}$$

and $\mathbf{0}$ is all-zero vector or matrix. The interpolation problem has a unique solution with the assumption that φ is conditionally positive definite of order ℓ , and the node set X is $\Psi_{\ell-1}$ -unisolvent. We define cardinal basis functions $s_1, \dots, s_{n_{\text{loc}}^i} \in \mathcal{R}_i$ w.r.t the stencil nodes in X_i , i.e., $s_j(x_{i_k}) = \delta_{jk}$, where δ_{jk} is the Kronecker delta. Then, the interpolation function s_u can be expressed as

$$s_u(x) = \sum_{j=1}^{n_{\text{loc}}^i} u(x_{i_j}) s_j(x).$$

The differential operator \mathcal{L} on s_u at some $x_i \in X$ is given by

$$\mathcal{L}s_u(x_i) = \sum_{j=1}^{n_{\text{loc}}^i} u(x_{i_j}) \mathcal{L}s_j(x_i). \quad (2.4)$$

Compared (2.4) with (2.2), the weights can be computed by $w_j^i := \mathcal{L}s_j(x_i)$. By the linear system (2.3) and the definition of s_j , we have

$$s_j(x) = \left[\varphi_{\epsilon, x_{i_1}}(x), \dots, \varphi_{\epsilon, x_{i_{n_{\text{loc}}^i}}}(x), p_1(x), \dots, p_Q(x) \right] (\tilde{A}^i)^{-1} \begin{bmatrix} e_j \\ \mathbf{0} \end{bmatrix},$$

where $e_j \in \mathbb{R}^n$ denotes the j -th unit vector. Hence, define

$$\mathcal{L}\Phi^i = \left[\mathcal{L}\varphi_{\epsilon, x_{i_1}}(x_i), \dots, \mathcal{L}\varphi_{\epsilon, x_{i_{n_{\text{loc}}^i}}}(x_i) \right], \quad \mathcal{L}\mathbf{p}^i = \left[\mathcal{L}p_1(x_i), \dots, \mathcal{L}p_Q(x_i) \right],$$

then we obtain

$$\begin{bmatrix} w_1^i, \dots, w_{n_{\text{loc}}^i}^i \end{bmatrix} = \left[\mathcal{L}\Phi^i, \mathcal{L}\mathbf{p}^i \right] (\tilde{A}^i)^{-1} \begin{bmatrix} I_{n_{\text{loc}}^i} \\ \mathbf{0} \end{bmatrix},$$

where $I_{n_{\text{loc}}^i} \in \mathbb{R}^{n_{\text{loc}}^i \times n_{\text{loc}}^i}$ is the identity matrix.

Augmentation of the matrix on the right to an $(n_{\text{loc}}^i + Q) \times (n_{\text{loc}}^i + Q)$ identity matrix and introduction of dummy variables \tilde{w}_j^i (which may later be discarded since they originated from the arbitrary augmentation to the identity matrix) leads to the linear system of equations

$$\tilde{A}^i \begin{bmatrix} w^i \\ \tilde{w}^i \end{bmatrix} = \begin{bmatrix} \mathcal{L}\Phi^i \\ \mathcal{L}\mathbf{p}^i \end{bmatrix} \quad (2.5)$$

where

$$w^i := [w_1^i, \dots, w_{n_{\text{loc}}^i}^i]^T, \quad \tilde{w}^i := [\tilde{w}_1^i, \dots, \tilde{w}_Q^i]^T$$

for the desired stencil weights w_j^i in the approximation (2.2). Without polynomial augmentation, (2.5) simplifies to $A^i w^i = \mathcal{L}\Phi^i$.

Now we apply the RBF-FD method to the discretization of a linear partial differential equation with Dirichlet boundary condition

$$\begin{cases} \mathcal{L}u(x) = f(x), & x \in \Omega, \\ u(x) = g(x), & x \in \partial\Omega. \end{cases} \quad (2.6)$$

For each interior node $x_i \in X_\Omega$, we compute a stencil $X_i \subset X$ of size n_{loc}^i and stencil weights w^i by solving (2.5). The stencil weights are used to compute u_i to approximate $u(x_i)$ where u is the solution of (2.6), i.e., $u_i \approx u(x_i)$ at all interior nodes $x_i \in X_\Omega$, by enforcing equality in (2.2),

$$\sum_{j=1}^{n_{\text{loc}}^i} w_j^i u(x_{i_j}) = f(x_i), \quad i \in \{1, \dots, N_I\}. \quad (2.7)$$

From (2.6), we have $u_{i_j} = g(x_{i_j})$ for all $x_{i_j} \in \partial\Omega$. By substituting the Dirichlet boundary data from (2.6) into (2.7), we obtain

$$\sum_{\substack{j \in \{1, \dots, n_{\text{loc}}^i\} \\ \text{s.t. } x_{i_j} \in \Omega}} w_{i_j} u_{i_j} = f(x_i) - \sum_{\substack{j \in \{1, \dots, n_{\text{loc}}^i\} \\ \text{s.t. } x_{i_j} \in \partial\Omega}} w_{i_j} g(x_{i_j}) =: \tilde{f}_i, \quad i \in \{1, \dots, N_I\}.$$

Hence, we define the right hand side vector $\tilde{\mathbf{f}} := (\tilde{f}_1, \dots, \tilde{f}_{N_I})^T \in \mathbb{R}^{N_I}$ and the global stiffness matrix $L^I \in \mathbb{R}^{N_I \times N_I}$, containing the row-wise weights of the interior nodes of the i -th stencil,

$$L_{i,k}^I := \begin{cases} w_{i_j} & \exists j \in \{1, \dots, n_{\text{loc}}^i\} \text{ such that } x_k = x_{i_j} \text{ is in the stencil } X_i, \\ 0 & \text{otherwise.} \end{cases}$$

Then, the approximation can be computed by the following linear system

$$L^I \mathbf{u}^I = \tilde{\mathbf{f}},$$

where $\mathbf{u}^I = (u_1, \dots, u_{N_I})^T$ is the discretized approximated solution on interior nodes. This linear system can also contain the boundary nodes and be expressed in a more compact form

$$\left[\begin{array}{c|c} L & \\ \hline \mathbf{0} & I_{N-N_I} \end{array} \right] \begin{bmatrix} \mathbf{u}_I \\ \mathbf{u}_B \end{bmatrix} = \begin{bmatrix} \mathbf{f} \\ \mathbf{g} \end{bmatrix}, \quad (2.8)$$

where I_{N-N_I} is the identity matrix, L is defined in the same way as L^I , $\mathbf{u}^B = (u_{N_I+1}, \dots, u_N)^T$, $\mathbf{f} = (f(x_1), \dots, f(x_{N_I}))^T$, and $\mathbf{g} = (g(x_{N_I+1}), \dots, g(x_N))^T$. The discretized approximated solution $\mathbf{u} = (\mathbf{u}_I^T, \mathbf{u}_B^T)^T$ is the so-called high-fidelity solution in the context of RBM.

2.3 POD-based RBM

To construct a reduced order model for parametric PDEs, we sample n_s parameter samples $\Xi = \{\mu^1, \dots, \mu^{n_s}\}$ from the parameter space and computed the associated high-fidelity snapshots $\{\mathbf{u}_{\mu^1}, \dots, \mathbf{u}_{\mu^{n_s}}\}$ by (2.8). We define the snapshot matrix $S \in \mathbb{R}^{N \times n_s}$ as $S = [\mathbf{u}_{\mu^1} | \dots | \mathbf{u}_{\mu^{n_s}}]$. The SVD decomposition of S reads

$$S = U \Sigma Z^T,$$

where $U = [\zeta_1 | \dots | \zeta_N] \in \mathbb{R}^{N \times N}$ and $Z = [\psi_1 | \dots | \psi_{n_s}] \in \mathbb{R}^{n_s \times n_s}$ are orthogonal matrices, and $\Sigma = \text{diag}(\sigma_1, \dots, \sigma_r) \in \mathbb{R}^{N \times n_s}$ with $\sigma_1 \geq \sigma_2 \geq \dots \geq \sigma_r > 0$, where the rank $r \leq \min(N, n_s)$.

For any $n_{\text{POD}} \leq n_s$, the first n_{POD} left singular vectors $\zeta_1, \dots, \zeta_{n_{\text{POD}}}$, associated with the largest n_{POD} singulars of U , form the POD basis $V \in \mathbb{R}^{N \times n_{\text{POD}}}$ of dimension n_{POD} . We have the following important result.

Proposition 1. [16, Proposition 6.1.] *Let*

$$\mathcal{W}_{n_{\text{POD}}} = \{W \in \mathbb{R}^{N \times n_{\text{POD}}} : W^T W = I_N\}$$

be the set of all n_{POD} -dimensional orthonormal basis. Then,

$$\sum_{i=1}^{n_s} \|\mathbf{u}_{\mu^i} - VV^T \mathbf{u}_{\mu^i}\|_2^2 = \min_{W \in \mathcal{W}_{n_{\text{POD}}}} \sum_{i=1}^{n_s} \|\mathbf{u}_{\mu^i} - WW^T \mathbf{u}_{\mu^i}\|_2^2 = \sum_{i=n_{\text{POD}}+1}^r \sigma_i^2 \quad (2.9)$$

Hence, the POD basis captures the main part of the snapshot matrix and guarantees a minimal projection-recovery error among the selected snapshots. This error also equals the square sum of the tail of the singular values. From this perspective, we can also choose a desired error tolerance $\varepsilon_{\text{POD}} > 0$ and calculate the POD dimension n_{POD} by

$$n_{\text{POD}} := \min \left\{ n \in \mathbb{N} \mid \frac{\sum_{i=1}^n \sigma_i^2}{\sum_{i=1}^r \sigma_i^2} \geq 1 - \varepsilon_{\text{POD}}^2 \right\}.$$

Then for any new $\mu \in \mathcal{D}$, we can approximate \mathbf{u}_{μ} by a span of the POD basis, i.e.,

$$\mathbf{u}_{\mu} \approx \sum_{i=1}^{n_{\text{POD}}} c_i(\mu) \zeta_i.$$

Substitute this equation into (2.8), we have

$$\sum_{i=1}^{n_{\text{POD}}} c_i(\mu) \left[\begin{array}{c|c} L(\mu) & \\ \mathbf{0} & I_{N-N_I} \end{array} \right] \zeta_i = \begin{bmatrix} \mathbf{f}(\mu) \\ \mathbf{g}(\mu) \end{bmatrix},$$

or an equivalent form

$$\begin{aligned} B_{\mu} \mathbf{c}_{\mu} &:= \begin{bmatrix} \mathbf{f}(\mu) \\ \mathbf{g}(\mu) \end{bmatrix}, \\ B_{\mu} &:= \left[\left[\begin{array}{c|c} L(\mu) & \\ \mathbf{0} & I_{N-N_I} \end{array} \right] \zeta_1, \dots, \left[\begin{array}{c|c} L(\mu) & \\ \mathbf{0} & I_{N-N_I} \end{array} \right] \zeta_{n_{\text{POD}}} \right], \end{aligned} \quad (2.10)$$

where $B_{\mu} \in \mathbb{R}^{N \times n_{\text{POD}}}$, $\mathbf{c}_{\mu} \in \mathbb{R}^{n_{\text{POD}}}$. This is typically an overdetermined system and we seek a least square solution, which is given by the Moore-Penrose inverse

$$B_{\mu}^{\dagger} = (B_{\mu}^T B_{\mu})^{-1} B_{\mu}^T. \quad (2.11)$$

Here, we assume that the POD basis is well-chosen such that B_{μ} is column full-rank. The least square solution reads

$$\mathbf{c}_{\mu} = B_{\mu}^{\dagger} \begin{bmatrix} \mathbf{f}(\mu) \\ \mathbf{g}(\mu) \end{bmatrix}. \quad (2.12)$$

In the previous description, POD is applied to the reduced order model for parametrized PDEs. By (2.9), the POD basis is the n_{POD} -dimensional basis which best approximates the set of solution snapshots $\{\mathbf{u}_{\mu^1}, \dots, \mathbf{u}_{\mu^{n_s}}\}$. There remain two questions unanswered:

- the approximation property of the POD basis with respect to all the admissible solutions $\{\mathbf{u}_\mu : \mu \in \mathcal{D}\}$ associated with the parameter space.
- how to select the number and sites of the samples $\Xi = \{\mu^1, \dots, \mu^{n_s}\}$ so that the snapshots set is sufficiently representative of all the admissible solutions.

For the first question, readers could follow [16, Chapter 5] and the references therein. To address the second issue, it is necessary to use a continuous form of POD, by introducing a measure on \mathcal{D} and consider the integral version of the minimization problem in (2.9):

$$\min_{W \in \mathcal{W}_{n_{\text{POD}}}} \int_{\mathcal{D}} \|\mathbf{u}_\mu - WW^T \mathbf{u}_\mu\|_2^2 d\mu.$$

This minimization problem can be solved by introducing a suitable quadrature formula to approximate the integrals, which leads to an improved POD algorithm with quadrature weights. The POD technique can also be generalized to minimize the energy norm associated with the high-fidelity solution space, rather than the $\|\cdot\|_2$ norm of the snapshots vectors. As our work computes the snapshot by the collocation RBF method, we only consider the $\|\cdot\|_2$ norm. The design of the quadratures weights also exceeds the scope of this paper and we recommend readers to refer to [16] for more details. In our numerical analysis, we will adopt the vanilla POD model and, to a certain degree, answer the second question through the lens of numerical experimentation.

3 Numerical Algorithm

Our algorithm operates in two distinct phases: an offline phase and an online phase. In the offline phase, we leverage the POD method to produce the reduced basis and integrate it in the training of neural networks, which require the bulk of the computational workload. This setup enables the online phase to simultaneously and efficiently simulate solutions for a vast array of parameters, a feat achieved through the synergistic exploitation of neural network parallelism and matrix computations. Our algorithm demonstrates superior efficacy compared to the approach described by [1], which employs a similar offline-online decomposition strategy but without training neural networks. For a detailed numerical comparison, refer to Section 5.

In the offline phase, we generate the data set and train the neural network with this data set. We first discretize the domain Ω to get N nodes in the interior of Ω and on the boundary $\partial\Omega$. The RBF method is mesh-free and, therefore, suitable for irregular geometries. However, the accuracy of this method is heavily influenced by the discretization method. Generally, a set of nodes that allows low interpolation error cannot have a large region in Ω without centers, which means a small fill distance. Many practical methods can produce well-distributed node sets. Readers may refer to [4] for a geometric greedy method and see [1] for an alternative description.

After the discretization, the RBF-FD method is ready to calculate a high-fidelity ground truth solution, or snapshot \mathbf{u}_μ given any $\mu \in \mathcal{D}$. By sampling the parameter space of n_s parameter samples, we calculate the snapshots matrix $S \in \mathbb{R}^{N \times n_s}$. Then, we choose the tolerance value ε_{POD} and calculate the POD basis $V \in \mathbb{R}^{N \times n_{\text{POD}}}$ by the SVD decomposition. Here, we also need to consider the values of n_s , ε_{POD} , and the location of the samples $\{\mu^1, \dots, \mu^{n_s}\}$.

The choices of $n_s, \varepsilon_{\text{POD}}$ must balance the accuracy and computation time. The location of the samples should be well-distributed and representative. One may consider a uniform tensorial sampling with different grid step sizes in different dimensions, while other types of sparse grids are also possible. Different sizes and locations of $\{\mu^1, \dots, \mu^{n_s}\}$ do not necessarily having a significant impact on S and n_{POD} , which depends on the nature of the equation. The key is to ensure that the problem is suitable for the use of the RBM and reducible with the POD method. To verify that, we can check if the decay of the singular values of S is sufficiently fast. If the rates of decay are essentially the same for different values of n_s and locations of samples, a smaller n_s and simpler sampling method will be more favored. See our numerical example in Section 5 and a more detailed discussion in [16].

For any $\mu \in \mathcal{D}$, we solve the PDE (2.1) with RBF-FD (2.8) and obtain the coefficient vector $V^T \mathbf{u}_\mu \in \mathbb{R}^{n_{\text{POD}}}$ under the POD basis, which represents a parametric mapping $\mathcal{D} \rightarrow \mathbb{R}^{n_{\text{POD}}}$. Again, we sample another n_{data} points in \mathcal{D} to calculate the input-output pairs $\{(\mu^i, V^T \mathbf{u}_{\mu^i})\}_{i=1}^{n_{\text{data}}}$, and train the neural networks to approximate this mapping. We note that, compared with the numerical algorithm presented in [6] and [12], the use of POD in our algorithm or other possible reduced basis methods, can greatly reduce the output dimension of the neural network from N to n_{POD} , which is beneficial for networks training convergence, reduction in network sizes and training time.

In the online phase, prediction can be made in parallel given multiple parameters $\{\mu^1, \dots, \mu^n\}$. We only need to conduct one forward propagation through the neural network, denoted by **NN**, and multiply the POD basis, which gives the prediction $V\text{NN}([\mu^1 | \dots | \mu^n]) \in \mathbb{R}^{N \times n}$. We outline the entire algorithm in Algorithm 1.

Algorithm 1 POD-DNN algorithm for parametric PDEs

The offline phase

- 1: Discretize the domain Ω to get N nodes, and discretize the parameter space \mathcal{D} by $\{\mu^1, \dots, \mu^{n_s}\}$.
- 2: **for** $i = 1, \dots, n_s$ **do**
- 3: Use RBF-FD (2.8) to solve the PDE (2.1) with parameter μ^i , obtain high-fidelity solution \mathbf{u}_{μ^i} .
- 4: **end for**
- 5: Concatenate the snapshot matrix $S = [\mathbf{u}_{\mu^1}, \dots, \mathbf{u}_{\mu^{n_s}}]$.
- 6: Perform SVD on S to calculate the POD basis matrix V with tolerance ε_{POD} .
- 7: Sample another n_{data} points $\{\mu^1, \dots, \mu^{n_{\text{data}}}\}$ in \mathcal{D} .
- 8: **for** $i = 1, \dots, n_{\text{data}}$ **do**
- 9: Use RBF-FD (2.8) to solve the PDE (2.1) with parameter μ^i , obtain high-fidelity solution \mathbf{u}_{μ^i} and coefficient vector $V^T \mathbf{u}_{\mu^i}$.
- 10: **end for**
- 11: Save the input-output pairs $\{(\mu^i, V^T \mathbf{u}_{\mu^i})\}_{i=1}^{n_{\text{data}}}$ as data set.
- 12: Train the network **NN** with the data set.

The online phase

- 1: Given multiple parameters $\{\mu^1, \dots, \mu^n\}$, calculate $V\text{NN}([\mu^1 | \dots | \mu^n])$.
-

4 Theoretic Analysis

In this section, we first introduce the mathematical definition of deep ReLU networks, incorporating symbols and conventions that will be used consistently or referenced from the literature [11]. Additionally, we present some basic estimates in the form of lemmas. Subsequently, we will provide the proof of the main theorem.

4.1 Basic Definitions and Estimates

We first introduce concatenation and parallelization operations for neural networks, which may be used to construct complex neural networks from simple networks. Furthermore, we derive the complexity estimates of operations of ReLU neural networks.

Definition 1. Let $L, n_0 \in \mathbb{N}$. A neural network Φ with input dimension n_0 and number of layers $L = L(\Phi)$ is a matrix-vector sequence

$$\Phi = ((W_1, b_1), \dots, (W_L, b_L)),$$

where $W_i \in \mathbb{R}^{n_i \times n_{i-1}}$ are weight matrices, $b_i \in \mathbb{R}^{n_i}$ are bias vectors, and $n_i \in \mathbb{N}$ are width. Let $\sigma : \mathbb{R} \rightarrow \mathbb{R}$ be ReLU activation function, i.e., $\sigma(x) = \max\{0, x\}$. We define the realization of the network

$$R(\Phi) : \mathbb{R}^{n_0} \rightarrow \mathbb{R}^{n_L}, \quad R(\Phi)(x) = x_L,$$

where x_L is expressed as follows:

$$\begin{cases} x_0 := x, \\ x_i := \sigma(W_i x_{i-1} + b_i), \quad i = 1, 2, \dots, L-1, \\ x_L := W_L x_{L-1} + b_L, \end{cases}$$

where the ReLU function σ operates on the vector in an element-wise manner. Define the number of non-zero parameters in i -th layer $M_i(\Phi) := \|W_i\|_0 + \|b_i\|_0$ and the total number of non-zero parameters $M(\Phi) := \sum_{i=1}^L M_i(\Phi)$.

Next, we define the concatenation of two neural networks.

Definition 2. Let $L_1, L_2 \in \mathbb{N}$ and let $\Phi^1 = ((W_1^1, b_1^1), \dots, (W_{L_1}^1, b_{L_1}^1))$, $\Phi^2 = ((W_1^2, b_1^2), \dots, (W_{L_2}^2, b_{L_2}^2))$ be two neural networks with activation function σ . The input dimension of Φ^1 is the same as the output dimension of Φ^2 . Next, we denote $\Phi^1 \circ \Phi^2$ as the concatenation of Φ^1, Φ^2 as follows:

$$\begin{aligned} \Phi^1 \circ \Phi^2 := & \left((W_1^2, b_1^2), \dots, (W_{L_2-1}^2, b_{L_2-1}^2), \right. \\ & \left. (W_1^1 W_{L_2}^2, W_1^1 b_{L_2}^2 + b_1^1), (W_2^1, b_2^1), \dots, (W_{L_1}^1, b_{L_1}^1) \right), \end{aligned}$$

which yields $L(\Phi^1 \circ \Phi^2) = L_1 + L_2 - 1$.

Next lemma shows that $M(\Phi^1 \circ \Phi^2)$ can be estimated by $\max\{M(\Phi^1), M(\Phi^2)\}$ in some special cases.

Lemma 1. [11, Lemma A.1] Let Φ be a neural network with $L(\Phi)$ layers, n_0 -dimensional input and n_L -dimensional output. If $W \in \mathbb{R}^{1 \times n_L}$, then, for all $i = 1, \dots, L(\Phi)$,

$$M_i(((W, \mathbf{0})) \circ \Phi) \leq M_i(\Phi).$$

In particular, $M((W, \mathbf{0}) \circ \Phi) \leq M(\Phi)$. Moreover, if $W \in \mathbb{R}^{n_0 \times n}$ such that, for every $i \leq n_0$ there is at most one non-zero element in the i -th row $W_{i,:}$, then, for all $i = 1, \dots, L(\Phi)$,

$$M_i(\Phi \circ ((W, \mathbf{0}))) \leq M_i(\Phi).$$

In particular, $M(\Phi \circ ((W, \mathbf{0}))) \leq M(\Phi)$.

However, there is no bound on $M(\Phi^1 \circ \Phi^2)$ that is linear in $M(\Phi^1)$ and $M(\Phi^2)$ in general case. Hence we introduce an alternative sparse concatenation to control the number of non-zero parameters. We need the following lemma to construct the ReLU neural network of the identity function.

Lemma 2. [11, Lemma 3.3] For any $n, L \in \mathbb{N}$, there exists a neural network $\Phi_{n,L}^{\mathbf{Id}}$ with input dimension n and output dimension n such that

$$\begin{aligned} R(\Phi_{n,L}^{\mathbf{Id}}) &= \mathbf{Id}_{\mathbb{R}^n}, \\ M(\Phi_{n,L}^{\mathbf{Id}}) &\leq 2nL, \end{aligned}$$

and all the non-zero parameters are $\{-1, 1\}$ -valued.

Definition 3. Let Φ^1, Φ^2 be two neural networks such that the output dimension of Φ^2 and the input dimension of Φ^1 equal $n \in \mathbb{N}$. Then, the sparse concatenation of Φ^1 and Φ^2 is defined as

$$\Phi^1 \odot \Phi^2 := \Phi^1 \circ \Phi_{n,1}^{\mathbf{Id}} \circ \Phi^2$$

We now introduce the parallelization operation.

Definition 4. If Φ^1, \dots, Φ^k are neural networks that have equal input dimension and number of layers, such that $\Phi^i = ((W_1^i, b_1^i), \dots, (W_L^i, b_L^i))$. We define the parallelization of Φ^1, \dots, Φ^k with

$$P(\Phi^1, \dots, \Phi^k) := ((W_1, b_1), \dots, (W_L, b_L)),$$

where

$$W_i := \begin{pmatrix} W_i^1 & & & \\ & W_i^2 & & \\ & & \ddots & \\ & & & W_i^k \end{pmatrix}, \quad b_i := \begin{pmatrix} b_i^1 \\ b_i^2 \\ \vdots \\ b_i^k \end{pmatrix}, \quad i = 1, \dots, L.$$

If Φ^1, \dots, Φ^k are neural networks that have equal input dimensions but different numbers of layers. Let

$$L := \max \{L(\Phi^1), \dots, L(\Phi^k)\}$$

and we define the extension

$$E_L(\Phi^i) := \begin{cases} \Phi^i, & L(\Phi^i) = L, \\ \Phi_{n_{L(\Phi^i)}, L-L(\Phi^i)}^{\mathbf{Id}} \odot \Phi^i, & L(\Phi^i) < L, \end{cases}$$

where $n_{L(\Phi^i)}^i$ is the output dimension of Φ^i . We define the parallelization of Φ^1, \dots, Φ^k with

$$P(\Phi^1, \dots, \Phi^k) := P(E_L(\Phi^1), \dots, E_L(\Phi^k)).$$

The following two lemmas provide the properties of the sparse concatenation and the parallelization of neural networks.

Lemma 3. [11, Lemma 5.3] *Let Φ^1, Φ^2 be ReLU neural networks. The input dimension of Φ^1 equals the output dimension of Φ^2 . Then, for the sparse concatenation $\Phi^1 \odot \Phi^2$ it holds*

1. $R(\Phi^1)(R(\Phi^2)(\cdot)) = R(\Phi^1 \odot \Phi^2)(\cdot)$,
2. $L(\Phi^1 \odot \Phi^2) = L(\Phi^1) + L(\Phi^2)$,
3. $M(\Phi^1 \odot \Phi^2) \leq 2M(\Phi^1) + 2M(\Phi^2)$.

Lemma 4. [11, Lemma 5.4] *Let Φ^1, \dots, Φ^k be ReLU neural networks with equal input dimension n . Then, for the parallelization $P(\Phi^1, \dots, \Phi^k)$ it holds*

1. for all $x_1, \dots, x_k \in \mathbb{R}^n$,

$$R(P(\Phi^1, \dots, \Phi^k))(x_1, \dots, x_k) = (R(\Phi^1)(x_1), \dots, R(\Phi^k)(x_k)),$$

2. $L(P(\Phi^1, \dots, \Phi^k)) = \max\{L(\Phi^1), \dots, L(\Phi^k)\}$,
3. Let $n_{L(\Phi^i)}^i$ denote the output dimension of Φ^i , then

$$M(P(\Phi^1, \dots, \Phi^k)) \leq 2 \left(\sum_{i=1}^k M(\Phi^i) \right) + 4 \left(\sum_{i=1}^k n_{L(\Phi^i)}^i \right) \max_{i=1, \dots, k} L(\Phi^i),$$

4. $M(P(\Phi^1, \dots, \Phi^k)) = \sum_{i=1}^k M(\Phi^i)$, if $L(\Phi^1) = \dots = L(\Phi^k)$.

4.2 Neural Network Approximation of the Parametric Map

To approximate the parametric mapping $\mu \mapsto \mathbf{c}(\mu)$ using deep ReLU neural networks, we tackle the problem in two steps: first, approximating the inverse of a matrix, and second, approximating matrix multiplication. Initially, we present the concept of vectorized matrices to maintain the classical setup of the neural network.

Definition 5. *Let $A \in \mathbb{R}^{n \times k}$. We denote*

$$\text{vec}(A) := (A_{1,1}, \dots, A_{n,1}, \dots, A_{1,k}, \dots, A_{n,k})^T \in \mathbb{R}^{nk}.$$

Moreover, for a vector $v = (v_{1,1}, \dots, v_{n,1}, \dots, v_{1,k}, \dots, v_{n,k})^T \in \mathbb{R}^{nk}$, we set

$$\text{matr}(v) := (v_{i,j})_{i=1, \dots, n, j=1, \dots, k} \in \mathbb{R}^{n \times k}.$$

We give the following lemmas for approximating matrix multiplication with ReLU neural networks.

Lemma 5. [11, Proposition 3.7] Let $m, n, k \in \mathbb{N}$, $Z > 0$, and $\varepsilon \in (0, 1)$. There exists a ReLU neural network $\Phi_{\text{mult};\varepsilon}^{Z,m,n,k}$ with $n(m+k)$ -dimensional input, mk -dimensional output such that, for a universal constant $C_{\text{mult}} > 0$, we have

1. $\sup_{\substack{A \in \mathbb{R}^{m \times n}, B \in \mathbb{R}^{n \times k}, \\ \|A\|_2 \leq Z, \|B\|_2 \leq Z}} \left\| AB - \text{matr} \left(R \left(\Phi_{\text{mult};\varepsilon}^{Z,m,n,k} \right) (\text{vec}(A), \text{vec}(B)) \right) \right\|_2 \leq \varepsilon,$
2. $L \left(\Phi_{\text{mult};\varepsilon}^{Z,m,n,k} \right) \leq C_{\text{mult}} \cdot \left(\log_2(1/\varepsilon) + \log_2(n\sqrt{mk}) + \log_2(\max\{1, Z\}) \right),$
3. $M \left(\Phi_{\text{mult};\varepsilon}^{Z,m,n,k} \right) \leq C_{\text{mult}} mnk \cdot \left(\log_2(1/\varepsilon) + \log_2(n\sqrt{mk}) + \log_2(\max\{1, Z\}) \right).$

Lemma 6. [11, Proposition A.3] Let $n, i \in \mathbb{N}$, $Z > 0$, $\varepsilon \in (0, 1/4)$ and $\delta \in (0, 1)$. There exists a ReLU neural network $\Phi_{2^i;\varepsilon}^{1-\delta,n}$ with n^2 -dimensional input, n^2 -dimensional output such that, for a universal constant $C_{\text{sq}} > 0$, we have

1. $\sup_{A \in \mathbb{R}^{n \times n}, \|A\|_2 \leq 1-\delta} \left\| A^{2^i} - \text{matr} \left(R \left(\Phi_{2^i;\varepsilon}^{1-\delta,n} \right) (\text{vec}(A)) \right) \right\|_2 \leq \varepsilon,$
2. $L \left(\Phi_{2^i;\varepsilon}^{1-\delta,n} \right) \leq C_{\text{sq}} i \cdot \left(\log_2(1/\varepsilon) + \log_2 n + i \right),$
3. $M \left(\Phi_{2^i;\varepsilon}^{1-\delta,n} \right) \leq C_{\text{sq}} i n^3 \cdot \left(\log_2(1/\varepsilon) + \log_2 n + i \right).$

For the inverse operator, we prove the following proposition. By leveraging a different expansion form of the Neumann series, we improve the bound of the number of non-zero parameters, compared with a similar result in [11, Theorem 3.8].

Proposition 2. For $\varepsilon, \delta \in (0, 1)$, we define

$$l = l(\varepsilon, \delta) := \left\lceil \log_2 \left(\log_{1-\delta} \left(\frac{1}{2} \delta \varepsilon \right) + 1 \right) \right\rceil,$$

There exists a universal constant $C_{\text{inv}} > 0$ such that for every $n \in \mathbb{N}$, $\varepsilon \in (0, 1/4)$ and $\delta \in (0, 1)$, there exists a ReLU neural network $\Phi_{\text{inv};\varepsilon}^{1-\delta,n}$ with n^2 -dimensional input and n^2 -dimensional output satisfying the following properties:

1. $\sup_{A \in \mathbb{R}^{n \times n}, \|A\|_2 \leq 1-\delta} \left\| (I_n - A)^{-1} - \text{matr} \left(R \left(\Phi_{\text{inv};\varepsilon}^{1-\delta,n} \right) (\text{vec}(A)) \right) \right\|_2 \leq \varepsilon,$
2. $L \left(\Phi_{\text{inv};\varepsilon}^{1-\delta,n} \right) \leq C_{\text{inv}} l \cdot \left(\log_2(1/\varepsilon) + \log_2(1/\delta) + \log_2 n + l \right),$
3. $M \left(\Phi_{\text{inv};\varepsilon}^{1-\delta,n} \right) \leq C_{\text{inv}} 2^l n^2 (n + l) \cdot \left(\log_2(1/\varepsilon) + \log_2(1/\delta) + \log_2 n + l \right).$

Proof. Based on the properties of the partial sums of the Neumann series, for every $\varepsilon, \delta \in (0, 1)$ and $A \in \mathbb{R}^{n \times n}$ satisfying $\|A\|_2 \leq 1 - \delta$, we have

$$\left\| (I_n - A)^{-1} - \sum_{i=0}^{2^l-1} A^i \right\|_2 = \left\| (I_n - A)^{-1} A^{2^l} \right\|_2 \leq \frac{1}{1 - (1 - \delta)} \cdot (1 - \delta)^{2^l} \leq \frac{\varepsilon}{2}.$$

Thus, it suffices to construct a ReLU neural network representing the partial sums. Note that

$$\sum_{i=0}^{2^l-1} A^i = \prod_{i=0}^{l-1} (A^{2^i} + I_n).$$

Let $Z_1 := 1 - \delta, Z_2 := 3 + \varepsilon + 1/\delta$. For $i = 1, \dots, l$, define $\Phi^1 := ((I_{n^2}, \text{vec}(I_{n^2})))$,

$$\Pi^i := \begin{cases} \Phi^1, & i = 1, \\ \Phi_{\text{mult}; 5^{i-l-1}\varepsilon/2}^{Z_2, n, n, n} \odot P \left(\Pi^{i-1}, \Phi^1 \odot \Phi_{2^{i-1}; 5^{i-l-1}\delta\varepsilon/2}^{Z_1, n} \right), & i \geq 2, \end{cases}$$

and

$$\Phi^i := \Pi^i \circ \left(\left(\begin{pmatrix} I_{n^2} \\ \vdots \\ I_{n^2} \end{pmatrix}, \mathbf{0} \right) \right),$$

where I_{n^2} repeats i times. We claim that, for $i = 1, \dots, l$, we have

$$\left\| \text{matr} (R(\Phi^i) (\text{vec}(A))) - \sum_{k=0}^{2^i-1} A^k \right\|_2 \leq \frac{\varepsilon}{2 \cdot 5^{l-i}}.$$

We prove this by induction. The case $i = 1$ is trivial. If the claim holds for $i' = 1, \dots, i - 1$, then

$$\begin{aligned} & \left\| \text{matr} (R(\Phi^i) (\text{vec}(A))) - \sum_{k=0}^{2^i-1} A^k \right\|_2 \\ & \leq \left\| \sum_{k=0}^{2^i-1} A^k - \left(\text{matr} \left(R \left(\Phi_{2^{i-1}; 5^{i-l-1}\delta\varepsilon/2}^{Z_1, n} \right) (\text{vec}(A)) \right) + I_n \right) \prod_{k=0}^{i-2} (A^{2^k} + I_n) \right\|_2 \\ & \quad + \left\| \left(\text{matr} \left(R \left(\Phi_{2^{i-1}; 5^{i-l-1}\delta\varepsilon/2}^{Z_1, n} \right) (\text{vec}(A)) \right) + I_n \right) \prod_{k=0}^{i-2} (A^{2^k} + I_n) \right. \\ & \quad \left. - \left(\text{matr} \left(R \left(\Phi_{2^{i-1}; 5^{i-l-1}\delta\varepsilon/2}^{Z_1, n} \right) (\text{vec}(A)) \right) + I_n \right) \text{matr} (R(\Phi^{i-1}) (\text{vec}(A))) \right\|_2 \\ & \quad + \left\| \left(\text{matr} \left(R \left(\Phi_{2^{i-1}; 5^{i-l-1}\delta\varepsilon/2}^{Z_1, n} \right) (\text{vec}(A)) \right) + I_n \right) \text{matr} (R(\Phi^{i-1}) (\text{vec}(A))) \right. \\ & \quad \left. - \text{matr} (R(\Phi^i) (\text{vec}(A))) \right\|_2 \\ & := \mathbf{I} + \mathbf{II} + \mathbf{III} \end{aligned}$$

For term **I**, by Lemma 6 we have

$$\mathbf{I} \leq \left\| \sum_{k=0}^{2^{i-1}-1} A^k \right\|_2 \cdot 5^{i-l-1}\delta\varepsilon/2 \leq 5^{i-l-1}\varepsilon/2.$$

For term **II**, by induction we have

$$\mathbf{II} \leq \left\| \text{matr} \left(R \left(\Phi_{2^{i-1}; 5^{i-l-1}\delta\varepsilon/2}^{Z_1, n} \right) (\text{vec}(A)) \right) + I_n \right\|_2 \cdot 5^{i-l-1}\varepsilon/2 \leq 3 \cdot 5^{i-l-1}\varepsilon/2.$$

For term **III**, by Lemma 5 we have $\mathbf{III} \leq 5^{i-l-1}\varepsilon/2$. Combining **I**, **II** and **III**, we have proven the claim. Let $\Phi_{\text{inv};\varepsilon}^{1-\delta,n} := \Phi^l$, then this ReLU neural network satisfies the error estimate of the proposition.

Next, we analyze the size of the resulting neural network Φ^l by induction. For all $i = 1, \dots, l$, by Lemma 3, Lemma 4, Lemma 5 and Lemma 6, we have

$$\begin{aligned} L(\Phi^i) &= L(\Pi^i) \\ &\leq L(\Phi_{\text{mult};5^{i-l-1}\varepsilon/2}^{Z_2,n,n,n}) + \max\{L(\Pi^{i-1}), L(\Phi_{2^{i-1};5^{i-l-1}\delta\varepsilon/2}^{Z_1,n}) + 1\} \\ &\leq C_{\text{mult}} \cdot (\log_2(1/\varepsilon) + l + \log_2 n + \log_2(\max\{1, Z_2\})) \\ &\quad + \max\{C_{\text{sq}}(i-1) \cdot (\log_2(1/\varepsilon) + \log_2(1/\delta) + \log_2 n + l), L(\Pi^{i-1})\}. \end{aligned}$$

Let $C_0 := 2C_{\text{mult}} + C_{\text{sq}}$. Note that $L(\Pi^1) \leq C_0 \cdot (\log_2(1/\varepsilon) + \log_2(1/\delta) + \log_2 n + l)$. By induction we have

$$L(\Phi^i) \leq C_0 i \cdot (\log_2(1/\varepsilon) + \log_2(1/\delta) + \log_2 n + l).$$

By Lemma 1, Lemma 3, Lemma 4, Lemma 5 and Lemma 6, we have

$$\begin{aligned} M(\Phi^i) &\leq M(\Pi^i) \\ &\leq 2M(\Phi_{\text{mult};5^{i-l-1}\varepsilon/2}^{Z_2,n,n,n}) + 2M(\Pi^{i-1}) + 4M(\Phi^1) + 4M(\Phi_{2^{i-1};5^{i-l-1}\delta\varepsilon/2}^{Z_1,n}) \\ &\quad + 8n^2 \max\{L(\Pi^{i-1}), L(\Phi_{2^{i-1};5^{i-l-1}\delta\varepsilon/2}^{Z_1,n}) + 1\} \\ &\leq 2M(\Pi^{i-1}) + 2C_{\text{mult}}n^3 \cdot (\log_2(1/\varepsilon) + l + \log_2 n + \log_2(\max\{1, Z_2\})) \\ &\quad + 4C_{\text{sq}}(i-1)n^3 \cdot (\log_2(1/\varepsilon) + \log_2(1/\delta) + \log_2 n + l) \\ &\quad + 8C_0(i-1)n^2 \cdot (\log_2(1/\varepsilon) + \log_2(1/\delta) + \log_2 n + l). \end{aligned}$$

Let $C_1 := 4C_{\text{sq}} + 8C_0$. By induction we have

$$\begin{aligned} M(\Phi^i) &\leq 2^i n^2 + 2^i C_{\text{mult}} n^3 \cdot (\log_2(1/\varepsilon) + l + \log_2 n + \log_2(1/\delta)) \\ &\quad + 2^i i C_1 n^2 \cdot (\log_2(1/\varepsilon) + \log_2(1/\delta) + \log_2 n + l). \end{aligned}$$

With a suitable chosen $C_{\text{inv}} > 0$, we have completed the proof. \square

Recall that the coefficient vector under the reduced basis is calculated by

$$\mathbf{c}_\mu = (B_\mu^T B_\mu)^{-1} B_\mu^T \begin{bmatrix} \mathbf{f}(\mu) \\ \mathbf{g}(\mu) \end{bmatrix},$$

where $B_\mu \in \mathbb{R}^{N \times n_{\text{POD}}}$ is defined by (2.10). We now approximate the mapping $\mu \mapsto \mathbf{c}_\mu$ using ReLU neural networks. We have already shown that ReLU neural networks can approximate the inverse and multiplication operators. It remains to assume that the mappings $\mu \mapsto (\mathbf{f}(\mu), \mathbf{g}(\mu))^T, \mu \mapsto B_\mu$ can also be approximated by ReLU neural networks. Hence, we introduce the following assumptions.

Assumption 1. *The spectrum $\Lambda(B_\mu^T B_\mu) \subset [\beta^2, \alpha^2]$ with $0 < \beta^2 < \alpha^2$ for all $\mu \in \mathcal{D}$ and possible reduced basis V . The norm $\|(\mathbf{f}(\mu), \mathbf{g}(\mu))^T\|_2 \leq \gamma$ with $\gamma > 0$ for all $\mu \in \mathcal{D}$.*

Assumption 2. For any $\varepsilon > 0$ and reduced basis $V = [\zeta_1, \dots, \zeta_{n_{\text{POD}}}] \in \mathbb{R}^{N \times n_{\text{POD}}}$, there exists a ReLU neural network $\Phi_{V,\varepsilon}^B$ with p -dimensional input and Nn_{POD} -dimensional output such that

$$\sup_{\mu \in \mathcal{D}} \|B_\mu - \text{matr}(R(\Phi_{V,\varepsilon}^B)(\mu))\|_2 \leq \varepsilon,$$

which implies another ReLU neural network $\Phi_{V,\varepsilon}^{B^T}$ such that

$$\sup_{\mu \in \mathcal{D}} \|B_\mu^T - \text{matr}(R(\Phi_{V,\varepsilon}^{B^T})(\mu))\|_2 \leq \varepsilon.$$

We set $L(B; V, \varepsilon) := L(\Phi_{V,\varepsilon}^B) = L(\Phi_{V,\varepsilon}^{B^T})$ and $M(B; V, \varepsilon) := M(\Phi_{V,\varepsilon}^B) = M(\Phi_{V,\varepsilon}^{B^T})$.

Assumption 3. For any $\varepsilon > 0$, there exists a ReLU neural network $\Phi_\varepsilon^{\text{fg}}$ with p -dimensional input and N -dimensional output such that

$$\sup_{\mu \in \mathcal{D}} \|(\mathbf{f}(\mu), \mathbf{g}(\mu))^T - R(\Phi_\varepsilon^{\text{fg}})(\mu)\|_2 \leq \varepsilon.$$

We set $L(\mathbf{fg}; \varepsilon) := L(\Phi_\varepsilon^{\text{fg}})$ and $M(\mathbf{fg}; \varepsilon) := M(\Phi_\varepsilon^{\text{fg}})$.

Here, we remark that these assumptions can be fulfilled in a variety of cases. Recall the definition of B_μ in (2.10), we note that approximating the mapping $\mu \mapsto B_\mu$ is essentially equivalent to approximating the mapping of stiffness matrix $\mu \mapsto L(\mu)$, which in turn is tantamount to approximating $\mu \mapsto \mathcal{L}(\mu)\varphi_{\varepsilon,y}(x)$ and $\mu \mapsto \mathcal{L}(\mu)p_i(x)$. These mappings, together with $\mu \mapsto (\mathbf{f}(\mu), \mathbf{g}(\mu))^T$ in (3), can be easily constructed or approximated by neural networks if the parameter dependency of the parametric PDE (2.1) exhibits a simple form, such as a linear or rational nature. See [11] for some concrete examples.

By Proposition 2, we can apply $\Phi_{\text{inv};\varepsilon}^{1-\delta, n_{\text{POD}}}$ on $\text{vec}(I_{n_{\text{POD}}} - B_\mu^T B_\mu)$ to approximate $(B_\mu^T B_\mu)^{-1}$ if $\|I_{n_{\text{POD}}} - B_\mu^T B_\mu\|_2 \leq 1 - \delta$. To guarantee that, we introduce a scaling factor $\lambda > 0$ and ensure $\|I_{n_{\text{POD}}} - \lambda B_\mu^T B_\mu\|_2 \leq 1 - \delta$. Under Assumption 1, we can select $\lambda := (\alpha^2 + \beta^2)^{-1}$ and $\delta := \lambda\beta^2$, then $\|I_{n_{\text{POD}}} - \lambda(B_\mu^T B_\mu)\|_2 \leq 1 - \delta$ for all $\mu \in \mathcal{D}$ and possible reduced basis V . We fix values of λ and δ for the remainder of this paper. Now, we present the construction of the neural network to approximate $\mu \mapsto (B_\mu^T B_\mu)^{-1}$.

Proposition 3. Suppose that Assumption 1 and Assumption 2 hold. For any $\varepsilon \in (0, 1/4)$ and reduced basis $V \in \mathbb{R}^{N \times n_{\text{POD}}}$, there exists a ReLU neural network $\Phi_{\text{inv};\varepsilon}^{B^T B}$ with p -dimensional input and n_{POD}^2 -dimensional output that satisfies the following properties.

1. $\sup_{\mu \in \mathcal{D}} \|(B_\mu^T B_\mu)^{-1} - \text{matr}(R(\Phi_{\text{inv};\varepsilon}^{B^T B})(\mu))\|_2 \leq \varepsilon.$

2. There exists a constant C_L^B only depending on α and β , such that

$$\begin{aligned} L(\Phi_{\text{inv};\varepsilon}^{B^T B}) &\leq C_L^B \cdot \log_2(\log_2(1/\varepsilon)) \cdot (\log_2(1/\varepsilon) + \log_2 n_{\text{POD}}) \\ &\quad + C_L^B \log_2 N + L(B; V, \varepsilon_1), \end{aligned}$$

3. There exists a constant C_M^B only depending on α and β , such that

$$\begin{aligned} &M(\Phi_{\text{inv};\varepsilon}^{B^T B}) \\ &\leq C_M^B n_{\text{POD}}^2 \log_2(1/\varepsilon) \cdot (\log_2(\log_2(1/\varepsilon)) + n_{\text{POD}}) \cdot (\log_2(1/\varepsilon) + \log_2 n_{\text{POD}}) \\ &\quad + C_M^B N n_{\text{POD}}^2 \cdot (\log_2(1/\varepsilon) + \log_2 N) + 8M(B; V, \varepsilon_1). \end{aligned}$$

Here, $\varepsilon_1 := \min \left\{ \frac{\varepsilon \beta^4}{24\alpha}, \frac{\beta^2 \sqrt{\varepsilon}}{4}, \frac{\beta^2}{12\alpha}, \frac{\beta}{3} \right\}$.

Proof. Let $\varepsilon_1, \varepsilon_2 > 0$ be determined later. We define

$$\Phi_{\varepsilon_1, \varepsilon_2}^{B^T B} := \Phi_{\text{mult}; \varepsilon_2}^{\alpha + \varepsilon_1, n_{\text{POD}}, N, n_{\text{POD}}} \odot P \left(\Phi_{V, \varepsilon_1}^{B^T}, \Phi_{V, \varepsilon_1}^B \right) \circ \left(\left(\begin{pmatrix} \mathbf{I}_p \\ \mathbf{I}_p \end{pmatrix}, \mathbf{0} \right) \right).$$

By the triangle inequality, we have

$$\begin{aligned} & \sup_{\mu \in \mathcal{D}} \left\| B_\mu^T B_\mu - \text{matr} \left(R \left(\Phi_{\varepsilon_1, \varepsilon_2}^{B^T B} \right) (\mu) \right) \right\|_2 \\ & \leq \sup_{\mu \in \mathcal{D}} \left\| B_\mu^T B_\mu - B_\mu^T \text{matr} \left(R \left(\Phi_{V, \varepsilon_1}^B \right) (\mu) \right) \right\|_2 \\ & \quad + \sup_{\mu \in \mathcal{D}} \left\| B_\mu^T \text{matr} \left(R \left(\Phi_{V, \varepsilon_1}^B \right) (\mu) \right) - \text{matr} \left(R \left(\Phi_{V, \varepsilon_1}^{B^T} \right) (\mu) \right) \text{matr} \left(R \left(\Phi_{V, \varepsilon_1}^B \right) (\mu) \right) \right\|_2 \\ & \quad + \sup_{\mu \in \mathcal{D}} \left\| \text{matr} \left(R \left(\Phi_{V, \varepsilon_1}^{B^T} \right) (\mu) \right) \text{matr} \left(R \left(\Phi_{V, \varepsilon_1}^B \right) (\mu) \right) - \text{matr} \left(R \left(\Phi_{\varepsilon_1, \varepsilon_2}^{B^T B} \right) (\mu) \right) \right\|_2 \\ & =: \mathbf{I} + \mathbf{II} + \mathbf{III}. \end{aligned}$$

For term **I**, by Assumption 1 and Assumption 2 we have

$$\mathbf{I} \leq \sup_{\mu \in \mathcal{D}} \|B_\mu^T\|_2 \cdot \|B_\mu - \text{matr} \left(R \left(\Phi_{V, \varepsilon_1}^B \right) (\mu) \right)\|_2 \leq \alpha \varepsilon_1.$$

For term **II**, by Assumption 2 we have

$$\mathbf{II} \leq \sup_{\mu \in \mathcal{D}} \left\| B_\mu^T - \text{matr} \left(R \left(\Phi_{V, \varepsilon_1}^{B^T} \right) (\mu) \right) \right\|_2 \cdot \|\text{matr} \left(R \left(\Phi_{V, \varepsilon_1}^B \right) (\mu) \right)\|_2 \leq (\alpha + \varepsilon_1) \varepsilon_1.$$

For term **III**, note that $\|\text{matr} \left(R \left(\Phi_{V, \varepsilon_1}^B \right) (\mu) \right)\|_2$ and $\left\| \text{matr} \left(R \left(\Phi_{V, \varepsilon_1}^{B^T} \right) (\mu) \right) \right\|_2$ are below $(\alpha + \varepsilon_1)$. Hence we can use Lemma 5, which derives $\mathbf{III} \leq \varepsilon_2$. Then we can calculate the size of $\Phi_{\varepsilon_1, \varepsilon_2}^{B^T B}$. By Lemma 3, Lemma 4, Lemma 5, and Assumption 2, we have

$$\begin{aligned} & L(\Phi_{\varepsilon_1, \varepsilon_2}^{B^T B}) \\ & \leq L \left(\Phi_{\text{mult}; \varepsilon_2}^{\alpha + \varepsilon_1, n_{\text{POD}}, N, n_{\text{POD}}} \right) + \max \left\{ L \left(\Phi_{V, \varepsilon_1}^{B^T} \right), L \left(\Phi_{V, \varepsilon_1}^B \right) \right\} \\ & \leq C_{\text{mult}} \cdot (\log_2(1/\varepsilon_2) + \log_2(N n_{\text{POD}}) + \log_2(\max\{1, \alpha + \varepsilon_1\})) + L(B; V, \varepsilon_1). \end{aligned}$$

By Lemma 1, Lemma 3, Lemma 4, Lemma 5, and Assumption 2, we have

$$\begin{aligned} & M(\Phi_{\varepsilon_1, \varepsilon_2}^{B^T B}) \\ & \leq 2M \left(\Phi_{\text{mult}; \varepsilon_2}^{\alpha + \varepsilon_1, n_{\text{POD}}, N, n_{\text{POD}}} \right) + 4M(B; V, \varepsilon_1) \\ & \leq 2C_{\text{mult}} N n_{\text{POD}}^2 \cdot (\log_2(1/\varepsilon_2) + \log_2(N n_{\text{POD}}) + \log_2(\max\{1, \alpha + \varepsilon_1\})) \\ & \quad + 4M(B; V, \varepsilon_1). \end{aligned}$$

Now assume that $\Phi_{\varepsilon_1, \varepsilon_2}^{B^T B} = ((W_1, b_1), \dots, (W_L, b_L))$, we construct another ReLU neural network as

$$\Phi_{\varepsilon_1, \varepsilon_2}^{I - \lambda B^T B} := ((W_1, b_1), \dots, (-\lambda W_L, -\lambda b_L + \text{vec}(I_{n_{\text{POD}}}))).$$

We have

$$\begin{aligned}
& \sup_{\mu \in \mathcal{D}} \left\| I_{n_{\text{POD}}} - \lambda B_{\mu}^T B_{\mu} - \text{matr} \left(R \left(\Phi_{\varepsilon_1, \varepsilon_2}^{I - \lambda B^T B} \right) (\mu) \right) \right\|_2 \\
&= \sup_{\mu \in \mathcal{D}} \left\| I_{n_{\text{POD}}} - \lambda B_{\mu}^T B_{\mu} - \left(I_{n_{\text{POD}}} - \lambda \text{matr} \left(R \left(\Phi_{\varepsilon_1, \varepsilon_2}^{B^T B} \right) (\mu) \right) \right) \right\|_2 \\
&\leq \lambda (\mathbf{I} + \mathbf{II} + \mathbf{III}) \\
&\leq \lambda (2\alpha\varepsilon_1 + \varepsilon_1^2 + \varepsilon_2),
\end{aligned} \tag{4.1}$$

as well as

$$\begin{aligned}
L(\Phi_{\varepsilon_1, \varepsilon_2}^{I - \lambda B^T B}) &= L(\Phi_{\varepsilon_1, \varepsilon_2}^{B^T B}), \\
M(\Phi_{\varepsilon_1, \varepsilon_2}^{I - \lambda B^T B}) &\leq M(\Phi_{\varepsilon_1, \varepsilon_2}^{B^T B}) + n_{\text{POD}}.
\end{aligned} \tag{4.2}$$

As the final stage, we define the ReLU neural network

$$\Phi_{\text{inv}; \varepsilon_1, \varepsilon_2, \varepsilon_3}^{B^T B} := ((\lambda I_{n_{\text{POD}}}, \mathbf{0})) \circ \Phi_{\text{inv}; \varepsilon_3}^{1 - \delta/2, n_{\text{POD}}} \odot \Phi_{\varepsilon_1, \varepsilon_2}^{I - \lambda B^T B},$$

with p -dimensional input and n_{POD}^2 -dimensional output. The value $\varepsilon_3 > 0$ is undetermined. To bound the approximation error, we estimate

$$\begin{aligned}
& \sup_{\mu \in \mathcal{D}} \left\| (B_{\mu}^T B_{\mu})^{-1} - \text{matr} \left(R \left(\Phi_{\text{inv}; \varepsilon_1, \varepsilon_2, \varepsilon_3}^{B^T B} \right) (\mu) \right) \right\|_2 \\
&\leq \sup_{\mu \in \mathcal{D}} \left\| (B_{\mu}^T B_{\mu})^{-1} - \lambda \left(I_{n_{\text{POD}}} - \text{matr} \left(R \left(\Phi_{\varepsilon_1, \varepsilon_2}^{I - \lambda B^T B} \right) (\mu) \right) \right)^{-1} \right\|_2 \\
&\quad + \sup_{\mu \in \mathcal{D}} \left\| \lambda \left(I_{n_{\text{POD}}} - \text{matr} \left(R \left(\Phi_{\varepsilon_1, \varepsilon_2}^{I - \lambda B^T B} \right) (\mu) \right) \right)^{-1} \right. \\
&\quad \quad \left. - \lambda \text{matr} \left(R \left(\Phi_{\text{inv}; \varepsilon_3}^{1 - \delta/2, n_{\text{POD}}} \odot \Phi_{\varepsilon_1, \varepsilon_2}^{I - \lambda B^T B} \right) (\mu) \right) \right\|_2 \\
&=: \mathbf{IV} + \mathbf{V}.
\end{aligned} \tag{4.3}$$

For term \mathbf{IV} , using the equation $C^{-1} - D^{-1} = C^{-1}(D - C)D^{-1}$, we write

$$\begin{aligned}
\mathbf{IV} &\leq \sup_{\mu \in \mathcal{D}} \left\| (B_{\mu}^T B_{\mu})^{-1} \right\|_2 \cdot \left\| \lambda^{-1} \left(I_{n_{\text{POD}}} - \text{matr} \left(R \left(\Phi_{\varepsilon_1, \varepsilon_2}^{I - \lambda B^T B} \right) (\mu) \right) \right) - B_{\mu}^T B_{\mu} \right\|_2 \\
&\quad \cdot \left\| \lambda \left(I_{n_{\text{POD}}} - \text{matr} \left(R \left(\Phi_{\varepsilon_1, \varepsilon_2}^{I - \lambda B^T B} \right) (\mu) \right) \right)^{-1} \right\|_2.
\end{aligned}$$

Assumption 1 and (4.1) yields that

$$\sup_{\mu \in \mathcal{D}} \left\| \lambda^{-1} \left(I_{n_{\text{POD}}} - \text{matr} \left(R \left(\Phi_{\varepsilon_1, \varepsilon_2}^{I - \lambda B^T B} \right) (\mu) \right) \right) - B_{\mu}^T B_{\mu} \right\|_2 \leq 2\alpha\varepsilon_1 + \varepsilon_1^2 + \varepsilon_2,$$

and

$$\begin{aligned}
& \sup_{\mu \in \mathcal{D}} \left\| \lambda \left(I_{n_{\text{POD}}} - \text{matr} \left(R \left(\Phi_{\varepsilon_1, \varepsilon_2}^{I - \lambda B^T B} \right) (\mu) \right) \right)^{-1} \right\|_2 \\
&\leq \lambda / \left(\inf_{\mu \in \mathcal{D}} \left\| \lambda B_{\mu}^T B_{\mu} \right\|_2 - \lambda (2\alpha\varepsilon_1 + \varepsilon_1^2 + \varepsilon_2) \right) \\
&\leq (\beta^2 - (2\alpha\varepsilon_1 + \varepsilon_1^2 + \varepsilon_2))^{-1}.
\end{aligned}$$

Here, we shall make sure that $\beta^2 - (2\alpha\varepsilon_1 + \varepsilon_1^2 + \varepsilon_2) > 0$ when determine the values of $\varepsilon_1, \varepsilon_2$. Then term \mathbf{IV} can be bounded as

$$\mathbf{IV} \leq \beta^{-2} (2\alpha\varepsilon_1 + \varepsilon_1^2 + \varepsilon_2) (\beta^2 - (2\alpha\varepsilon_1 + \varepsilon_1^2 + \varepsilon_2))^{-1}.$$

For term \mathbf{V} , (4.1) yields that

$$\begin{aligned} \sup_{\mu \in \mathcal{D}} \left\| \text{matr} \left(R \left(\Phi_{\varepsilon_1, \varepsilon_2}^{I - \lambda B^T B} \right) (\mu) \right) \right\|_2 &\leq \lambda(2\alpha\varepsilon_1 + \varepsilon_1^2 + \varepsilon_2) + \sup_{\mu \in \mathcal{D}} \left\| I_{n_{\text{POD}}} - \lambda B_\mu^T B_\mu \right\|_2 \\ &\leq \lambda(2\alpha\varepsilon_1 + \varepsilon_1^2 + \varepsilon_2) + 1 - \lambda\beta^2. \end{aligned}$$

Assume that $\lambda(2\alpha\varepsilon_1 + \varepsilon_1^2 + \varepsilon_2) + 1 - \lambda\beta^2 \leq 1 - \delta/2$, then by Proposition 2, $\mathbf{V} \leq \lambda\varepsilon_3$. Combining \mathbf{IV} and \mathbf{V} implies

$$\begin{aligned} \sup_{\mu \in \mathcal{D}} \left\| (B_\mu^T B_\mu)^{-1} - \text{matr} \left(R \left(\Phi_{\text{inv}; \varepsilon_1, \varepsilon_2, \varepsilon_3}^{B^T B} \right) (\mu) \right) \right\|_2 \\ \leq \mathbf{IV} + \mathbf{V} \leq \beta^{-2}(2\alpha\varepsilon_1 + \varepsilon_1^2 + \varepsilon_2)(\beta^2 - (2\alpha\varepsilon_1 + \varepsilon_1^2 + \varepsilon_2))^{-1} + \lambda\varepsilon_3. \end{aligned} \quad (4.4)$$

For the size of neural network, by Lemma 3, Proposition 2 and (4.2), we have

$$\begin{aligned} &L(\Phi_{\text{inv}; \varepsilon_1, \varepsilon_2, \varepsilon_3}^{B^T B}) \\ &= L(\Phi_{\text{inv}; \varepsilon_3}^{1 - \delta/2, n_{\text{POD}}}) + L(\Phi_{\varepsilon_1, \varepsilon_2}^{B^T B}) \\ &\leq C_{\text{inv}} l(\varepsilon_3, \delta/2) (\log_2(1/\varepsilon_3) + l(\varepsilon_3, \delta/2) + \log_2(1/\delta) + \log_2(n_{\text{POD}})) \\ &\quad + C_{\text{mult}} \cdot (\log_2(1/\varepsilon_2) + \log_2(Nn_{\text{POD}}) + \log_2(\max\{1, \alpha + \varepsilon_1\})) + L(B; V, \varepsilon_1) \end{aligned}$$

and

$$\begin{aligned} &M(\Phi_{\text{inv}; \varepsilon_1, \varepsilon_2, \varepsilon_3}^{B^T B}) \\ &\leq 2M(\Phi_{\text{inv}; \varepsilon_3}^{1 - \delta/2, n_{\text{POD}}}) + 2M(\Phi_{\varepsilon_1, \varepsilon_2}^{B^T B}) + 2n_{\text{POD}} \\ &\leq 2C_{\text{inv}} 2^{l(\varepsilon_3, \delta/2)} n_{\text{POD}}^2 (n_{\text{POD}} + l(\varepsilon_3, \delta/2)) \\ &\quad \cdot (\log_2(1/\varepsilon_3) + l(\varepsilon_3, \delta/2) + \log_2(1/\delta) + \log_2(n_{\text{POD}})) \\ &\quad + 4C_{\text{mult}} N n_{\text{POD}}^2 \cdot (\log_2(1/\varepsilon_2) + \log_2(Nn_{\text{POD}}) + \log_2(\max\{1, \alpha + \varepsilon_1\})) \\ &\quad + 8M(B; V, \varepsilon_1) + 2n_{\text{POD}}. \end{aligned}$$

It remains to determine the values of $\varepsilon_1, \varepsilon_2, \varepsilon_3$. Recall that we should make sure

$$\beta^2 - (2\alpha\varepsilon_1 + \varepsilon_1^2 + \varepsilon_2) > 0, \quad \lambda(2\alpha\varepsilon_1 + \varepsilon_1^2 + \varepsilon_2) + 1 - \lambda\beta^2 \leq 1 - \delta/2.$$

Besides, the approximation error bound in the conclusion should hold, which can be proved by (4.4) if

$$\beta^{-2}(2\alpha\varepsilon_1 + \varepsilon_1^2 + \varepsilon_2)(\beta^2 - (2\alpha\varepsilon_1 + \varepsilon_1^2 + \varepsilon_2))^{-1} + \lambda\varepsilon_3 \leq \varepsilon.$$

One can check that the following values are sufficient.

$$\varepsilon_1 = \min \left\{ \frac{\varepsilon\beta^4}{24\alpha}, \frac{\beta^2\sqrt{\varepsilon}}{4}, \frac{\beta^2}{12\alpha}, \frac{\beta}{3} \right\}, \quad \varepsilon_2 = \min \left\{ \frac{\beta^4\varepsilon}{12}, \frac{\beta^2}{6} \right\}, \quad \varepsilon_3 = \frac{\varepsilon}{2\lambda}.$$

Let $\Phi_{\text{inv}; \varepsilon}^{B^T B} := \Phi_{\text{inv}; \varepsilon_1, \varepsilon_2, \varepsilon_3}^{B^T B}$ and plug in these values yields

$$\begin{aligned} \sup_{\mu \in \mathcal{D}} \left\| (B_\mu^T B_\mu)^{-1} - \text{matr} \left(R \left(\Phi_{\text{inv}; \varepsilon}^{B^T B} \right) (\mu) \right) \right\|_2 &\leq \frac{\varepsilon}{2} + \frac{\varepsilon}{2} \leq \varepsilon, \\ L(\Phi_{\text{inv}; \varepsilon}^{B^T B}) &\leq C_L^B \cdot \log_2(\log_2(1/\varepsilon)) \cdot (\log_2(1/\varepsilon) + \log_2 n_{\text{POD}}) + C_L^B \log_2 N + L(B; V, \varepsilon_1), \\ M(\Phi_{\text{inv}; \varepsilon}^{B^T B}) &\leq C_M^B n_{\text{POD}}^2 \log_2(1/\varepsilon) \cdot (\log_2(\log_2(1/\varepsilon)) + n_{\text{POD}}) \cdot (\log_2(1/\varepsilon) + \log_2 n_{\text{POD}}) \\ &\quad + C_M^B N n_{\text{POD}}^2 \cdot (\log_2(1/\varepsilon) + \log_2 N) + 8M(B; V, \varepsilon_1), \end{aligned}$$

where C_L^B and C_M^B are suitably chosen constants only depending on α and β . This completes the proof. \square

We can now construct ReLU neural networks that approximate the parametric map $\mu \mapsto \mathbf{c}(\mu)$. We present our main result.

Theorem 1. *Suppose that Assumption 1, Assumption 2 and Assumption 3 hold. For any $\varepsilon \in (0, 1/4)$ and reduced basis $V \in \mathbb{R}^{N \times n_{\text{POD}}}$, there exists a ReLU neural network $\Phi_{\text{para};\varepsilon}^{\mathbf{c}}$ with p -dimensional input and n_{POD} -dimensional output that satisfies the following properties.*

1. $\sup_{\mu \in \mathcal{D}} \|\mathbf{c}(\mu) - R(\Phi_{\text{para};\varepsilon}^{\mathbf{c}})(\mu)\|_2 \leq \varepsilon.$

2. *There exists a constant $C_L^{\mathbf{c}}$ only depending on α, β, γ , such that*

$$\begin{aligned} L(\Phi_{\text{para};\varepsilon}^{\mathbf{c}}) &\leq C_L^{\mathbf{c}} \cdot \log_2(\log_2(1/\varepsilon)) \cdot (\log_2(1/\varepsilon) + \log_2 n_{\text{POD}}) \\ &\quad + C_L^{\mathbf{c}} \log_2 N + L(B; V, \varepsilon_{4,1}) + L(B; V, \varepsilon_1) + L(\mathbf{fg}; \varepsilon_2), \end{aligned}$$

3. *There exists a constant $C_M^{\mathbf{c}}$ only depending on α, β, γ , such that*

$$\begin{aligned} &M(\Phi_{\text{para};\varepsilon_{1:5}}^{\mathbf{c}}) \\ &\leq C_M^{\mathbf{c}} N n_{\text{POD}}^2 \cdot (\log_2(1/\varepsilon) + \log_2 N) \\ &\quad + C_M^{\mathbf{c}} n_{\text{POD}}^2 \log_2(1/\varepsilon) \cdot (\log_2(\log_2(1/\varepsilon)) + n_{\text{POD}}) \cdot (\log_2(1/\varepsilon) + \log_2 n_{\text{POD}}) \\ &\quad + C_M^{\mathbf{c}} n_{\text{POD}}^2 \cdot \log_2(\log_2(1/\varepsilon)) \cdot \log_2 N \\ &\quad + 16M(B; V, \varepsilon_1) + 16M(\mathbf{fg}; \varepsilon_2) + 8M(B; V, \varepsilon_3) \\ &\quad + 80N n_{\text{POD}} L(B; V, \varepsilon_1) + 80N n_{\text{POD}} L(\mathbf{fg}; \varepsilon_2) + 16n_{\text{POD}}^2 L(B; V, \varepsilon_3). \end{aligned}$$

Here $\varepsilon_1 := \min \left\{ \frac{\varepsilon \beta^2}{12\gamma}, \frac{\beta \sqrt{\varepsilon}}{4}, \frac{\alpha}{4}, \frac{\sqrt{\alpha\gamma}}{2} \right\}$, $\varepsilon_2 := \min \left\{ \frac{\varepsilon \beta^2}{12\alpha}, \frac{\beta \sqrt{\varepsilon}}{4}, \frac{\gamma}{4}, \frac{\sqrt{\alpha\gamma}}{2} \right\}$ and $\varepsilon_3 := \min \left\{ \frac{\varepsilon \beta^4}{144\alpha^2\gamma}, \frac{\beta^2 \sqrt{6\alpha\gamma\varepsilon}}{24\alpha\gamma}, \frac{\beta^2}{12\alpha}, \frac{\beta}{3} \right\}$.

Proof. Let $\varepsilon_1, \varepsilon_2, \varepsilon_3, \varepsilon_4, \varepsilon_5, Z_1, Z_2 > 0$ be determined later. Let $\Phi_{V, \varepsilon_1}^{B^T}$ be the neural network defined in Assumption 2 and $\Phi_{\varepsilon_2}^{\mathbf{fg}}$ be the neural network defined in Assumption 3. We define

$$\Phi_{\varepsilon_1, \varepsilon_2, \varepsilon_3}^{B^T \mathbf{fg}} := \Phi_{\text{mult}; \varepsilon_3}^{Z_1, n_{\text{POD}}, N, 1} \odot P \left(\Phi_{V, \varepsilon_1}^{B^T}, \Phi_{\varepsilon_2}^{\mathbf{fg}} \right) \circ \left(\left(\begin{pmatrix} I_p \\ I_p \end{pmatrix}, \mathbf{0} \right) \right).$$

Let $\Phi_{\text{inv}; \varepsilon_4}^{B^T B}$ be the neural network derived in Proposition 3. We define

$$\Phi_{\text{para}; \varepsilon_{1:5}}^{\mathbf{c}} := \Phi_{\text{mult}; \varepsilon_5}^{Z_2, n_{\text{POD}}, n_{\text{POD}}, 1} \odot P \left(\Phi_{\text{inv}; \varepsilon_4}^{B^T B}, \Phi_{\varepsilon_1, \varepsilon_2, \varepsilon_3}^{B^T \mathbf{fg}} \right) \circ \left(\left(\begin{pmatrix} I_p \\ I_p \end{pmatrix}, \mathbf{0} \right) \right),$$

According to the triangle inequality, we obtain the estimation

$$\begin{aligned} &\sup_{\mu \in \mathcal{D}} \|\mathbf{c}(\mu) - R(\Phi_{\text{para}; \varepsilon_{1:5}}^{\mathbf{c}})(\mu)\|_2 \\ &\leq \sup_{\mu \in \mathcal{D}} \left\| (B_\mu^T B_\mu)^{-1} B_\mu^T (\mathbf{f}(\mu), \mathbf{g}(\mu))^T - (B_\mu^T B_\mu)^{-1} R(\Phi_{\varepsilon_1, \varepsilon_2, \varepsilon_3}^{B^T \mathbf{fg}})(\mu) \right\|_2 \\ &\quad + \sup_{\mu \in \mathcal{D}} \left\| (B_\mu^T B_\mu)^{-1} R(\Phi_{\varepsilon_1, \varepsilon_2, \varepsilon_3}^{B^T \mathbf{fg}})(\mu) - \text{matr} \left(R(\Phi_{\text{inv}; \varepsilon_4}^{B^T B})(\mu) R(\Phi_{\varepsilon_1, \varepsilon_2, \varepsilon_3}^{B^T \mathbf{fg}})(\mu) \right) \right\|_2 \\ &\quad + \sup_{\mu \in \mathcal{D}} \left\| \text{matr} \left(R(\Phi_{\text{inv}; \varepsilon_4}^{B^T B})(\mu) R(\Phi_{\varepsilon_1, \varepsilon_2, \varepsilon_3}^{B^T \mathbf{fg}})(\mu) \right) - R(\Phi_{\text{para}; \varepsilon_{1:5}}^{\mathbf{c}})(\mu) \right\|_2 \\ &=: \mathbf{I} + \mathbf{II} + \mathbf{III}. \end{aligned}$$

The term **I** can be further bounded by

$$\begin{aligned}
\mathbf{I} &\leq \sup_{\mu \in \mathcal{D}} \left\| (B_\mu^T B_\mu)^{-1} \right\|_2 \cdot \left(\left\| B_\mu^T (\mathbf{f}(\mu), \mathbf{g}(\mu))^T - B_\mu^T R \left(\Phi_{\varepsilon_2}^{\mathbf{f}\mathbf{g}} \right) (\mu) \right\|_2 \right. \\
&\quad + \left\| B_\mu^T R \left(\Phi_{\varepsilon_2}^{\mathbf{f}\mathbf{g}} \right) (\mu) - \text{matr} \left(R \left(\Phi_{V, \varepsilon_1}^{B^T} \right) (\mu) \right) R \left(\Phi_{\varepsilon_2}^{\mathbf{f}\mathbf{g}} \right) (\mu) \right\|_2 \\
&\quad + \left\| \text{matr} \left(R \left(\Phi_{V, \varepsilon_1}^{B^T} \right) (\mu) \right) R \left(\Phi_{\varepsilon_2}^{\mathbf{f}\mathbf{g}} \right) (\mu) - R \left(\Phi_{\varepsilon_1, \varepsilon_2, \varepsilon_3}^{B^T \mathbf{f}\mathbf{g}} \right) (\mu) \right\|_2 \Big) \\
&\leq \beta^{-2} (\mathbf{IV} + \mathbf{V} + \mathbf{VI}).
\end{aligned}$$

For term **IV** and **V**, Assumption 1, Assumption 2 and Assumption 3 yield $\mathbf{IV} \leq \alpha \varepsilon_2$, $\mathbf{V} \leq (\gamma + \varepsilon_2) \varepsilon_1$.

For term **VI**, we assume that

$$\begin{aligned}
\sup_{\mu \in \mathcal{D}} \left\| \text{matr} \left(R \left(\Phi_{V, \varepsilon_1}^{B^T} \right) (\mu) \right) \right\|_2 &\leq \alpha + \varepsilon_1 \leq Z_1, \\
\sup_{\mu \in \mathcal{D}} \left\| R \left(\Phi_{\varepsilon_2}^{\mathbf{f}\mathbf{g}} \right) (\mu) \right\|_2 &\leq \gamma + \varepsilon_2 \leq Z_1.
\end{aligned}$$

Then, by Lemma 5 we have $\mathbf{VI} \leq \varepsilon_3$.

For term **I**, combining the estimates above yields $\mathbf{I} \leq \beta^{-2} (\alpha \varepsilon_2 + (\gamma + \varepsilon_2) \varepsilon_1 + \varepsilon_3)$.

For term **II**, by the bound of term **IV**, **V** and **VI** we have

$$\begin{aligned}
\sup_{\mu \in \mathcal{D}} \left\| R \left(\Phi_{\varepsilon_1, \varepsilon_2, \varepsilon_3}^{B^T \mathbf{f}\mathbf{g}} \right) (\mu) \right\|_2 &\leq \mathbf{IV} + \mathbf{V} + \mathbf{VI} + \left\| B_\mu^T (\mathbf{f}(\mu), \mathbf{g}(\mu))^T \right\|_2 \\
&\leq \alpha \varepsilon_2 + (\gamma + \varepsilon_2) \varepsilon_1 + \varepsilon_3 + \alpha \gamma.
\end{aligned}$$

Hence, by Proposition 3 we have

$$\begin{aligned}
\mathbf{II} &\leq \sup_{\mu \in \mathcal{D}} \left\| (B_\mu^T B_\mu)^{-1} - \text{matr} \left(R \left(\Phi_{\text{inv}; \varepsilon_4}^{B^T B} \right) (\mu) \right) \right\|_2 \cdot \left\| R \left(\Phi_{\varepsilon_1, \varepsilon_2, \varepsilon_3}^{B^T \mathbf{f}\mathbf{g}} \right) (\mu) \right\|_2 \\
&\leq \varepsilon_4 (\alpha \varepsilon_2 + (\gamma + \varepsilon_2) \varepsilon_1 + \varepsilon_3 + \alpha \gamma).
\end{aligned}$$

For term **III**, we assume that

$$\begin{aligned}
\sup_{\mu \in \mathcal{D}} \left\| \text{matr} \left(R \left(\Phi_{\text{inv}; \varepsilon_4}^{B^T B} \right) (\mu) \right) \right\|_2 &\leq \varepsilon_4 + \beta^{-2} \leq Z_2, \\
\sup_{\mu \in \mathcal{D}} \left\| R \left(\Phi_{\varepsilon_1, \varepsilon_2, \varepsilon_3}^{B^T \mathbf{f}\mathbf{g}} \right) (\mu) \right\|_2 &\leq \alpha \varepsilon_2 + (\gamma + \varepsilon_2) \varepsilon_1 + \varepsilon_3 + \alpha \gamma \leq Z_2.
\end{aligned}$$

Then, by Lemma 5 we have $\mathbf{III} \leq \varepsilon_5$.

Combining these estimates yields

$$\begin{aligned}
\sup_{\mu \in \mathcal{D}} \left\| \mathbf{c}(\mu) - R \left(\Phi_{\text{para}; \varepsilon_{1:5}}^{\mathbf{c}} \right) (\mu) \right\|_2 &\leq \mathbf{I} + \mathbf{II} + \mathbf{III} \\
&\leq \beta^{-2} (\alpha \varepsilon_2 + (\gamma + \varepsilon_2) \varepsilon_1 + \varepsilon_3) + \varepsilon_4 (\alpha \varepsilon_2 + (\gamma + \varepsilon_2) \varepsilon_1 + \varepsilon_3 + \alpha \gamma) + \varepsilon_5.
\end{aligned}$$

Next, we estimate the size of the ReLU neural networks $\Phi_{\text{para};\varepsilon_{1:5}}^{\mathbf{c}}$. By Lemma 3, Lemma 4, Lemma 5 and Proposition 3, we have

$$\begin{aligned}
& L(\Phi_{\text{para};\varepsilon_{1:5}}^{\mathbf{c}}) \\
& \leq L(\Phi_{\text{mult};\varepsilon_5}^{Z_2, n_{\text{POD}}, n_{\text{POD}}, 1}) \\
& \quad + \max \left\{ L(\Phi_{\text{inv};\varepsilon_4}^{B^T B}), L(\Phi_{\text{mult};\varepsilon_3}^{Z_1, n_{\text{POD}}, N, 1}) + \max \left\{ L(\Phi_{V, \varepsilon_1}^{B^T}), L(\Phi_{\varepsilon_2}^{\mathbf{fg}}) \right\} \right\} \\
& \leq C_{\text{mult}} \cdot (\log_2(1/\varepsilon_5) + \log_2(n_{\text{POD}}\sqrt{n_{\text{POD}}}) + \log_2(\max\{1, Z_2\})) \\
& \quad + C_L^B \cdot \log_2(\log_2(1/\varepsilon_4)) \cdot (\log_2(1/\varepsilon_4) + \log_2 n_{\text{POD}}) \\
& \quad + C_L^B \log_2 N + L(B; V, \varepsilon_{4,1}) \\
& \quad + C_{\text{mult}} \cdot (\log_2(1/\varepsilon_3) + \log_2(N\sqrt{n_{\text{POD}}}) + \log_2(\max\{1, Z_1\})) \\
& \quad + L(B; V, \varepsilon_1) + L(\mathbf{fg}; \varepsilon_2),
\end{aligned}$$

where $\varepsilon_{4,1} := \min \left\{ \frac{\beta^4 \varepsilon_4}{24\alpha}, \frac{\beta^2}{12\alpha}, \frac{\sqrt{\varepsilon_4} \beta^2}{4}, \frac{\beta}{3} \right\}$, and

$$\begin{aligned}
& M(\Phi_{\text{para};\varepsilon_{1:5}}^{\mathbf{c}}) \\
& \leq 2M(\Phi_{\text{mult};\varepsilon_5}^{Z_2, n_{\text{POD}}, n_{\text{POD}}, 1}) + 4M(\Phi_{\text{inv};\varepsilon_4}^{B^T B}) \\
& \quad + 8M(\Phi_{\text{mult};\varepsilon_3}^{Z_1, n_{\text{POD}}, N, 1}) + 16M(\Phi_{V, \varepsilon_1}^{B^T}) + 16M(\Phi_{\varepsilon_2}^{\mathbf{fg}}) \\
& \quad + 32(Nn_{\text{POD}} + N) \max \left\{ L(\Phi_{V, \varepsilon_1}^{B^T}), L(\Phi_{\varepsilon_2}^{\mathbf{fg}}) \right\} \\
& \quad + 8(n_{\text{POD}}^2 + n_{\text{POD}}) \max \left\{ L(\Phi_{\text{inv};\varepsilon_4}^{B^T B}), L(\Phi_{\text{mult};\varepsilon_3}^{Z_1, n_{\text{POD}}, N, 1}) + \max \left\{ L(\Phi_{V, \varepsilon_1}^{B^T}), L(\Phi_{\varepsilon_2}^{\mathbf{fg}}) \right\} \right\} \\
& \leq 2C_{\text{mult}} n_{\text{POD}}^2 \cdot (\log_2(1/\varepsilon_5) + \log_2(n_{\text{POD}}\sqrt{n_{\text{POD}}}) + \log_2(\max\{1, Z_2\})) \\
& \quad + 4C_M^B n_{\text{POD}}^2 \log_2(1/\varepsilon_4) \cdot (\log_2(\log_2(1/\varepsilon_4)) + n_{\text{POD}}) \cdot (\log_2(1/\varepsilon_4) + \log_2 n_{\text{POD}}) \\
& \quad + 4C_M^B N n_{\text{POD}}^2 \cdot (\log_2(1/\varepsilon_4) + \log_2 N) + 8M(B; V, \varepsilon_{4,1}) \\
& \quad + 8C_{\text{mult}} N n_{\text{POD}} \cdot (\log_2(1/\varepsilon_3) + \log_2(N\sqrt{n_{\text{POD}}}) + \log_2(\max\{1, Z_1\})) \\
& \quad + 16M(B; V, \varepsilon_1) + 16M(\mathbf{fg}; \varepsilon_2) \\
& \quad + 64N n_{\text{POD}} L(B; V, \varepsilon_1) + 64N n_{\text{POD}} L(\mathbf{fg}; \varepsilon_2) + 16n_{\text{POD}}^2 L(B; V, \varepsilon_{4,1}) \\
& \quad + 16n_{\text{POD}}^2 C_L^B \log_2(\log_2(1/\varepsilon_4)) \cdot (\log_2(1/\varepsilon_4) + \log_2 n_{\text{POD}}) + 16n_{\text{POD}}^2 C_L^B \log_2 N \\
& \quad + 16n_{\text{POD}}^2 C_{\text{mult}} \cdot (\log_2(1/\varepsilon_3) + \log_2(N\sqrt{n_{\text{POD}}}) + \log_2(\max\{1, Z_1\})) \\
& \quad + 16n_{\text{POD}}^2 L(B; V, \varepsilon_1) + 16n_{\text{POD}}^2 L(\mathbf{fg}; \varepsilon_2).
\end{aligned}$$

It remains to determine the values of $\varepsilon_1, \dots, \varepsilon_5$. We have to guarantee that

$$\begin{aligned}
& \alpha + \varepsilon_1 \leq Z_1, \quad \gamma + \varepsilon_2 \leq Z_1, \quad \varepsilon_4 + \beta^{-2} \leq Z_2, \quad \alpha\varepsilon_2 + (\gamma + \varepsilon_2)\varepsilon_1 + \varepsilon_3 + \alpha\gamma \leq Z_2, \\
& \beta^{-2}(\alpha\varepsilon_2 + (\gamma + \varepsilon_2)\varepsilon_1 + \varepsilon_3) + \varepsilon_4(\alpha\varepsilon_2 + (\gamma + \varepsilon_2)\varepsilon_1 + \varepsilon_3 + \alpha\gamma) + \varepsilon_5 \leq \varepsilon,
\end{aligned}$$

which can be verified if

$$\begin{aligned}
& \varepsilon_1 = \min \left\{ \frac{\varepsilon\beta^2}{12\gamma}, \frac{\beta\sqrt{\varepsilon}}{4}, \frac{\alpha}{4}, \frac{\sqrt{\alpha\gamma}}{2} \right\}, \quad \varepsilon_2 = \min \left\{ \frac{\varepsilon\beta^2}{12\alpha}, \frac{\beta\sqrt{\varepsilon}}{4}, \frac{\gamma}{4}, \frac{\sqrt{\alpha\gamma}}{2} \right\}, \\
& \varepsilon_3 = \min \left\{ \frac{\varepsilon\beta^2}{12}, \frac{\alpha\gamma}{4} \right\}, \quad \varepsilon_4 = \frac{\varepsilon}{6\alpha\gamma}, \quad \varepsilon_5 = \frac{\varepsilon}{3}, \\
& Z_1 = \alpha + \gamma + \varepsilon_1 + \varepsilon_2, \quad Z_2 = \varepsilon_4 + \beta^{-2} + \alpha\varepsilon_2 + (\gamma + \varepsilon_2)\varepsilon_1 + \varepsilon_3 + \alpha\gamma.
\end{aligned}$$

Let $\Phi_{\text{para};\varepsilon}^{\mathbf{c}} := \Phi_{\text{para};\varepsilon_{1:5}}^{\mathbf{c}}$ and plug in these values yields

$$\begin{aligned} \sup_{\mu \in \mathcal{D}} \|\mathbf{c}(\mu) - \text{matr}(R(\Phi_{\text{para};\varepsilon_{1:5}}^{\mathbf{c}})(\mu))\|_2 &\leq \frac{\varepsilon}{3} + \frac{\varepsilon}{3} + \frac{\varepsilon}{3} \leq \varepsilon, \\ L(\Phi_{\text{para};\varepsilon}^{\mathbf{c}}) &\leq C_L^{\mathbf{c}} \cdot \log_2(\log_2(1/\varepsilon)) \cdot (\log_2(1/\varepsilon) + \log_2 n_{\text{POD}}) \\ &\quad + C_L^{\mathbf{c}} \log_2 N + L(B; V, \varepsilon_{4,1}) + L(B; V, \varepsilon_1) + L(\mathbf{fg}; \varepsilon_2), \\ M(\Phi_{\text{para};\varepsilon_{1:5}}^{\mathbf{c}}) &\leq C_M^{\mathbf{c}} N n_{\text{POD}}^2 \cdot (\log_2(1/\varepsilon) + \log_2 N) \\ &\quad + C_M^{\mathbf{c}} n_{\text{POD}}^2 \log_2(1/\varepsilon) \cdot (\log_2(\log_2(1/\varepsilon)) + n_{\text{POD}}) \cdot (\log_2(1/\varepsilon) + \log_2 n_{\text{POD}}) \\ &\quad + C_M^{\mathbf{c}} n_{\text{POD}}^2 \cdot \log_2(\log_2(1/\varepsilon)) \cdot \log_2 N \\ &\quad + 8M(B; V, \varepsilon_{4,1}) + 16M(B; V, \varepsilon_1) + 16M(\mathbf{fg}; \varepsilon_2) \\ &\quad + 80N n_{\text{POD}} L(B; V, \varepsilon_1) + 80N n_{\text{POD}} L(\mathbf{fg}; \varepsilon_2) + 16n_{\text{POD}}^2 L(B; V, \varepsilon_{4,1}), \end{aligned}$$

where $C_L^{\mathbf{c}}$ and $C_M^{\mathbf{c}}$ are suitably chosen constants only depending on α, β and γ . This completes the proof. \square

5 Numerical Experiments

In this section, we verify our analysis with numerical examples. We consider the two-dimensional Helmholtz equation in (28a) of [1].

$$\begin{cases} -u_{xx} - \mu_1 u_{yy} - \mu_2 u = -10 \sin(8x(y-1)), & (x, y) \in \Omega, \\ u = 0, & (x, y) \in \partial\Omega, \end{cases} \quad \mu \in \mathcal{D} = [0.1, 4] \times [0, 2], \quad (5.1)$$

where Ω , illustrated by Figure 1, is the interior of $\partial\Omega$ given by the polar coordinates equation $r(\theta) = 0.8 + 0.1(\sin(6\theta) + \sin(3\theta))$.

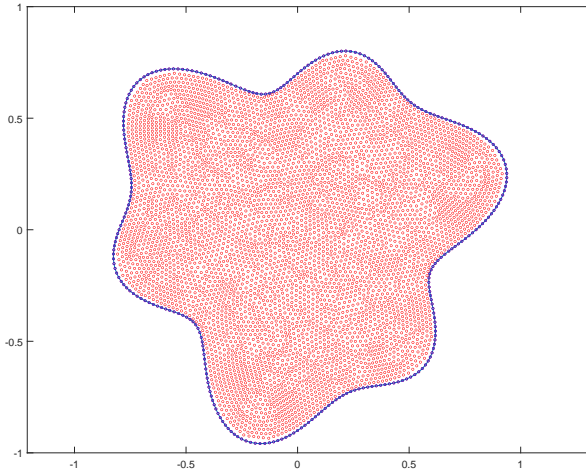


Figure 1: The irregular domain and discrete points on it.

5.1 Generating the Data Set

We follow Algorithm 1 to generate the data set. We choose the inverse multiquadrics (IMQ) $\varphi_\epsilon(r) = \frac{1}{\sqrt{1 + (\epsilon r)^2}}$ with shape parameter ϵ as the RBF. IMQ are positive definite functions and hence the stiffness matrix is calculated without polynomial augmentation. After shuffling and dividing the data set, we obtain n_{train} for training, n_{valid} for validation and $n_{\text{test}} = n_{\text{data}} - n_{\text{train}} - n_{\text{valid}}$ for testing.

The parameters are selected as follow: $N = 5731 = 5442 + 289 = N_I + N_B$, $\epsilon = 3$, $n_s = 100$ and $\varepsilon_{\text{POD}} = 10^{-6}$. This POD tolerance results in $n_{\text{POD}} = 20$. For the data set, $n_{\text{data}} = 10000 = 6000 + 2000 + 2000 = n_{\text{train}} + n_{\text{valid}} + n_{\text{test}}$.

Here, we give a brief discussion on our choices of the values of $n_s, \varepsilon_{\text{POD}}$. As we have mentioned in Section 3, we draw the spectrum decay of the snapshot matrix S to verify the reducibility of this equation under the POD method. Figure 2 illustrates the spectrum decay of S with $n_s = 25, 100, 400, 1600$, and the proportion of energy (i.e., the square sum of singulars) discarded under the corresponding truncation position. We confirm that in this problem, the decay speeds of singular values under different scenarios are essentially similar and sufficiently fast, which provides rationality for our choices of $n_s = 100, \varepsilon_{\text{POD}} = 10^{-6}$.

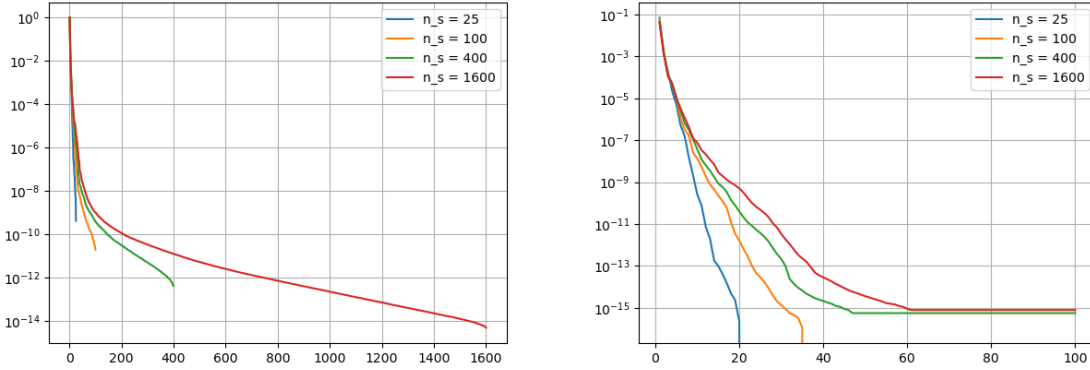


Figure 2: Left: The ratio of the singular values of S to the maximum singular value. Right: The proportion of energy discarded.

5.2 Structure of Neural Network

We use fully connected ReLU neural networks with L hidden layers and the width of layers as

$$(p = 2, n_{\text{neurons}}, \dots, n_{\text{neurons}}, n_{\text{POD}} = 20).$$

The ADAM optimizer with learning rate lr , $\beta_1 = 0.9$, $\beta_2 = 0.999$ and $\epsilon = 10^{-8}$ is used to train the networks. Each network is trained in n_{epochs} epochs. The loss function is the relative square error, defined as $\frac{\|\text{NN}(\mu) - V^T \mathbf{u}_\mu\|_2}{\|V^T \mathbf{u}_\mu\|_2}$. We choose the network with the best validation loss as the final model.

We need to determine some hyperparameters including L , n_{neurons} , n_{epochs} , lr and the batch size for batch gradient descent. To search for the optimal network architecture and training scheme, we perform a grid search with

$$L = 2, 4, 6, \quad n_{\text{neurons}} = 20, 100, 500, \quad n_{\text{epochs}} = 100, 1000, 5000, \\ \text{batch size} = 100, 1000, \quad \text{lr} = 0.01, 0.001, 0.0001.$$

We discovered that, in most cases, the network can achieve sufficient convergence when n_{epochs} is large enough (generally greater than 1000). A smaller batch size usually results in lower error, but also significantly increases training time. We show the test error and training time with $L = 2$, $n_{\text{neurons}} = 500$, lr = 0.0001 and different n_{epochs} , batch size in Table 1. Choosing depth L and width n_{neurons} shall balance the approximation ability and network complexity. We show the test error and training time with $n_{\text{epochs}} = 5000$, batch size = 100, lr = 0.0001 and different L , n_{neurons} in Table 2. Even though the optimal hyperparameters setting involves $n_{\text{epochs}} = 5000$, given that the network can achieve rapid convergence in the early stage of training, we can terminate the training during the middle phase of training by leveraging the early stopping technique, thus saving time. We found that halting the training between 1000-th to 2000-th epochs is usually appropriate. We show the loss history with the optimal hyperparameter setting in Figure 3. Combined with the optimal hyperparameters and early stopping technique, we conclude that $L = 2$, $n_{\text{neurons}} = 500$, $n_{\text{epochs}} = 2000$, batch size = 100, lr = 0.0001 is suitable for this problem and we will adopt this setting in the following experiments.

n_{epochs}	batch size	test error		training time(s)	
		100	1000	100	1000
100		0.00135	0.00561	12.026	5.402
1000		0.00087	0.00137	120.857	49.744
5000		0.00053	0.00120	573.608	260.685

Table 1: Test error and training time with different n_{epochs} and batch size.

L	n_{neurons}	test error			training time(s)		
		20	100	500	20	100	500
2		0.00517	0.00110	0.00053	615.729	642.774	573.608
4		0.00200	0.00066	0.00071	694.873	684.835	703.129
6		0.00286	0.00066	0.00082	804.566	795.738	818.161

Table 2: Test error and training time with different L and n_{neurons} .

5.3 Numerical Results and Comparisons

Here, we compare our POD-DNN model with Least Squares R²BFM (LS-R²BFM) in [1]. LS-R²BFM also adopts RBF-FD and an offline-online phase strategy. It constructs the reduced basis by a greedy algorithm. When the same number of reduced basis, $n_{\text{POD}} = n_{\text{Greedy}} = 20$, is chosen, Table 3 presents the average relative ℓ_2 error on the test set and the total inference

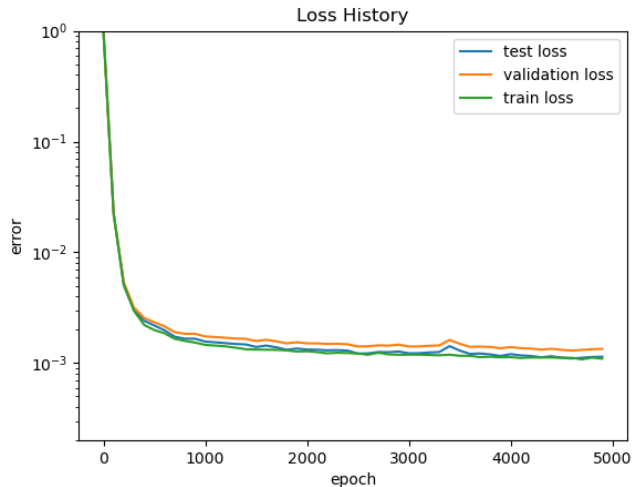


Figure 3: The loss history during training.

time for the two algorithms. Figure 4 displays the computed solutions and absolute errors. The solution from RBF-FD is taken as the ground truth for error computation, and its inference time is also presented as a reference. Unlike the other two algorithms, POD-DNN does not require solving any linear system during online inference after training. Besides, due to the easy parallelization of neural networks, our algorithm is very suitable for quick inference given multiple parameters. It significantly reduces inference time while maintaining accuracy equivalent to traditional methods.

The use of RBM significantly reduces the output dimension of DNNs from N to n_{POD} . This combination of RBM and DNN can be viewed as training the neural network with the output layer’s weight matrix fixed to the POD basis, which accelerates the convergence of the network during training.

	relative ℓ_2 error	inference time(s)
RBF-FD	/	3812.44900
LS-R ² BFM	0.00107	0.32587
POD-DNN	0.00148	0.00088

Table 3: The average relative ℓ_2 error and the total inference time on the test set.

6 Conclusions

In this paper, we propose the POD-DNN algorithm for solving parametric PDEs on irregular domains, which combines the RBF-FD method, POD-based RBM and DNN. RBM significantly reduces the cost of training neural networks, while neural networks further accelerate the computation in the online phase. Our main result (see Theorem 1) theoretically demonstrates that our algorithm is effective for approximating the parametric mapping, by showing that ReLU neural network can approximate the parametric map under accuracy ε with depth

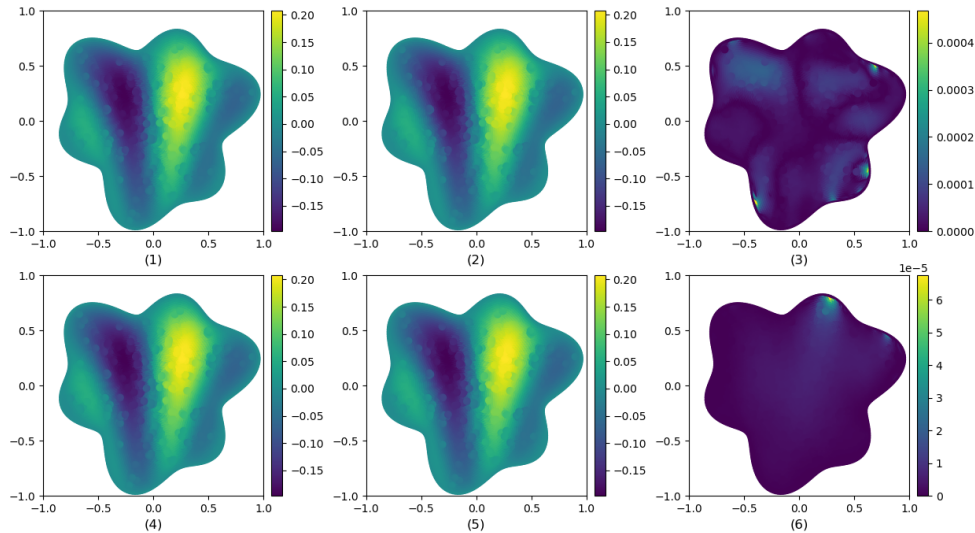


Figure 4: Computed solutions. (1-3): POD-DNN, RBF-FD and the absolute error. (4-6): R²BFM, RBF-FD and the absolute error.

$\mathcal{O}(\log_2(1/\varepsilon) \log_2(\log_2(1/\varepsilon)))$ and non-zero parameters $\mathcal{O}(n^3 \log_2^2(1/\varepsilon))$. For future research, both in computational and theoretical aspects, different structures of neural networks like convolutional neural networks could be designed to solve the parametric system.

References

- [1] Yanlai Chen, Sigal Gottlieb, Alfa Heryudono, and Akil Narayan. A reduced radial basis function method for partial differential equations on irregular domains. *J. Sci. Comput.*, 66(1):67–90, 2016.
- [2] Erik Adler Christensen., Morten Brøns, and Jens Nørkær Sørensen. Evaluation of proper orthogonal decomposition–based decomposition techniques applied to parameter-dependent nonturbulent flows. *SIAM J. Sci. Comput.*, 21(4):1419–1434, 1999.
- [3] Niccolò Dal Santo, Simone Deparis, and Luca Pegolotti. Data driven approximation of parametrized PDEs by reduced basis and neural networks. *J. Comput. Phys.*, 416:109550, 2020.
- [4] Stefano De Marchi, Robert Schaback, and Holger Wendland. Near-optimal data-independent point locations for radial basis function interpolation. *Adv. Comput. Math.*, 23(3):317–330, 2005.
- [5] Weinan E and Bing Yu. The deep Ritz method: A deep learning-based numerical algorithm for solving variational problems. *Commun. Math. Stat.*, 6(1):1–12, 2018.

- [6] Moritz Geist, Philipp Petersen, Mones Raslan, Reinhold Schneider, and Gitta Kutyniok. Numerical solution of the parametric diffusion equation by deep neural networks. *J. Sci. Comput.*, 88(1):22, 2021.
- [7] J. S. Hesthaven and S. Ubbiali. Non-intrusive reduced order modeling of nonlinear problems using neural networks. *J. Comput. Phys.*, 363:55–78, 2018.
- [8] Jan S. Hesthaven, Sigal Gottlieb, and David Gottlieb. *Spectral Methods for Time-Dependent Problems*, volume 21. Cambridge University Press, Cambridge, 2007.
- [9] Yuehaw Khoo, Jianfeng Lu, and Lexing Ying. Solving parametric pde problems with artificial neural networks. *European J. Appl. Math.*, 32(3):421–435, 2021.
- [10] K. Kunisch and S. Volkwein. Galerkin proper orthogonal decomposition methods for parabolic problems. *Numer. Math.*, 90(1):117–148, 2001.
- [11] Gitta Kutyniok, Philipp Petersen, Mones Raslan, and Reinhold Schneider. A theoretical analysis of deep neural networks and parametric PDEs. *Constr. Approx.*, 55(1):73–125, 2022.
- [12] Zhen Lei, Lei Shi, and Chenyu Zeng. Solving parametric partial differential equations with deep rectified quadratic unit neural networks. *J. Sci. Comput.*, 93(3):80, 2022.
- [13] Zongyi Li, Nikola Borislavov Kovachki, Kamyar Azizzadenesheli, Burigede Liu, Kaushik Bhattacharya, Andrew Stuart, and Anima Anandkumar. Fourier neural operator for parametric partial differential equations. In *International Conference on Learning Representations*, 2021.
- [14] Lu Lu, Pengzhan Jin, Guofei Pang, Zhongqiang Zhang, and George Em Karniadakis. Learning nonlinear operators via DeepONet based on the universal approximation theorem of operators. *Nat. Mach. Intell.*, 3(3):218–229, 2021.
- [15] C. Prud’homme, D. V. Rovas, K. Veroy, L. Machiels, Y. Maday, A. T. Patera, and G. Turinici. Reliable real-time solution of parametrized partial differential equations: Reduced-basis output bound methods. *J. Fluids Eng.*, 124(1):70–80, 2001.
- [16] Alfio Quarteroni, Andrea Manzoni, and Federico Negri. *Reduced Basis Methods for Partial Differential Equations*, volume 92. Springer, Cham, 2016.
- [17] M. Raissi, P. Perdikaris, and G. E. Karniadakis. Physics-informed neural networks: A deep learning framework for solving forward and inverse problems involving nonlinear partial differential equations. *J. Comput. Phys.*, 378:686–707, 2019.
- [18] Muruhan Rathinam and Linda R. Petzold. A new look at proper orthogonal decomposition. *SIAM J. Numer. Anal.*, 41(5):1893–1925, 2003.
- [19] Justin Sirignano and Konstantinos Spiliopoulos. DGM: A deep learning algorithm for solving partial differential equations. *J. Comput. Phys.*, 375:1339–1364, 2018.
- [20] Rohit K. Tripathy and Ilias Billionis. Deep UQ: Learning deep neural network surrogate models for high dimensional uncertainty quantification. *J. Comput. Phys.*, 375:565–588, 2018.
- [21] Holger Wendland. *Scattered Data Approximation*. Cambridge University Press, Cambridge, 2004.